NOTICE: The copyright law of the United States (Title 17, U.S. Code) governs the making of photocopies or other reproductions of copyrighted material. Under certain conditions specified in the law, libraries and archives are authorized to furnish a photocopy or other reproduction. One of these specified conditions is that the photocopy or reproduction is not to be "used for any purpose other than private study, scholarship, or research."

The CDC library absorbs the cost of copyright fees charged by publishers when applicable and the cost of articles and books obtained from other libraries. Copyright fees average $35.00 and fees charged by the lending libraries are between $10 and $15 per request

SAR and QSAR in Environmental Research
Vol. 22, Nos. 1–2, January–March 2011, 129–169

Taylor & Francis
Taylor & Francis Group

QSARs for PBPK modelling of environmental contaminants†

T. Peyret and K. Krishnan*

Département de santé environnementale et santé au travail, Université de Montréal, Montréal, Canada

(*Received 28 July 2010; in final form 12 November 2010*)

Physiologically-based pharmacokinetic (PBPK) models are increasingly finding use in risk assessment applications of data-rich compounds. However, it is a challenge to determine the chemical-specific parameters for these models, particularly in time- and resource-limiting situations. In this regard, SARs, QSARs and QPPRs are potentially useful for computing the chemical-specific input parameters of PBPK models. Based on the frequency of occurrence of molecular fragments (CH_3, CH_2, CH, C, C=C, H, benzene ring and H in benzene ring structure) and exposure conditions, the available QSAR-PBPK models facilitate the simulation of tissue and blood concentrations for some inhaled volatile organic chemicals. The application domain of existing QSARs for developing PBPK models is limited, due to lack of relevant data for diverse chemicals and mechanisms. Even though this approach is conceptually applicable to non-volatile and high molecular weight organics as well, it is more challenging to predict the other PBPK model parameters required for modelling the kinetics of these chemicals (particularly tissue diffusion coefficients, association constants for binding and oral absorption rates). As the level of our understanding of the mechanistic basis of toxicokinetic processes improves, QSARs to provide *a priori* predictions of key chemical-specific PBPK parameters can be developed to expedite the internal dose-based health risk assessments in data-poor situations.

Keywords: PBPK modelling; QSAR-PBPK; pharmacokinetics; *in silico*

Downloaded by [Montana State University Bozeman] at 08:07 20 August 2014

1. Introduction

Molecular structure-based prediction of the temporal change in the concentration of environmental chemicals or their metabolites in blood and organs of exposed organisms is a challenge. Even though several investigators reported the development of quantitative structure–property relationship (QSPR) models for certain pharmacokinetic parameters (e.g. volume of distribution, half-life) of anaesthetics and pharmaceuticals [1–3], there are few efforts on the QSAR-based prediction of the pharmacokinetic or toxicokinetic profiles of chemicals. The pharmaceutical literature consists of numerous examples of 2-D QSARs, 3-D QSARs and expert systems for modelling the individual components or phases of drug disposition and pharmacokinetics (i.e. absorption, distribution, metabolism and

*Corresponding author. Email: kannan.krishnan@umontreal.ca
†Presented at the 14th International Workshop on Quantitative Structure–Activity Relationships in Environmental and Health Sciences (QSAR2010), 24–28 May 2010, Montreal, Canada.

ISSN 1062–936X print/ISSN 1029–046X online
© 2011 Taylor & Francis
DOI: 10.1080/1062936X.2010.548351
http://www.informaworld.com

Downloaded by [Montana State University Bozeman] at 08:07 20 August 2014

elimination; ADME). Several reviews and reports present the advantages and limitations of the currently available algorithms and software for *in silico* modelling of the drug dissolution/bioavailability, oral absorption rate/fraction, volume of distribution, pathways, affinities or rates of metabolism, renal excretion rate as well as affinity for specific transporters [3–20]. These QSPRs for pharmacokinetic parameters and individual ADME processes could not be and have not been used in predictive toxicology, particularly in risk assessment, for providing *a priori* predictions of the time-course of the tissue or blood concentrations of the toxic moiety in intact animals and humans exposed to varying doses of chemicals by various routes and scenarios. Furthermore, the development of QSARs for each sampling point, dose, route and species would be an arduous task. However, *a priori* predictions can be obtained by developing QSPRs for the chemical-specific input parameters of mechanism-based models such as the physiologically-based pharmacokinetic (or toxicokinetic) models.

Physiologically-based pharmacokinetic (PBPK) modelling refers to the development and evaluation of mathematical descriptions of the ADME of chemicals in biota based on proven/hypothetical mechanistic determinants [21]. PBPK models essentially represent a systems biology approach to the study of ADME and are increasingly finding use in screening-level as well as quantitative risk assessments to reduce the uncertainties associated with interspecies, route-to-route, and high-dose to low-dose extrapolations of tissue dose of chemicals [21–24]. These models represent the organism as a set of several tissue compartments interconnected by blood flows (Figures 1 and 2). The compartments correspond to individual organs or groups of organs exhibiting the same time-course behaviour, as simulated by solving sets of mass-balance differential equations [21]. Examples of equations commonly used in PBPK models for simulating the pharmacokinetics of inhaled volatile organic chemicals (VOCs) are listed in Table 1. The input parameters required for solving the set of PBPK model equations are either species-specific or chemical-specific. The species-specific parameters, for example, relate to alveolar ventilation rate (Qp), cardiac output (Qc), tissue blood flow rates (Qt) and tissue volumes (Vt). The chemical-specific input parameters include partition coefficients (blood:air (P_{ba}), tissue:air (P_{ta}) or tissue:blood (P_{tb})) as well as metabolic parameters such as the maximal

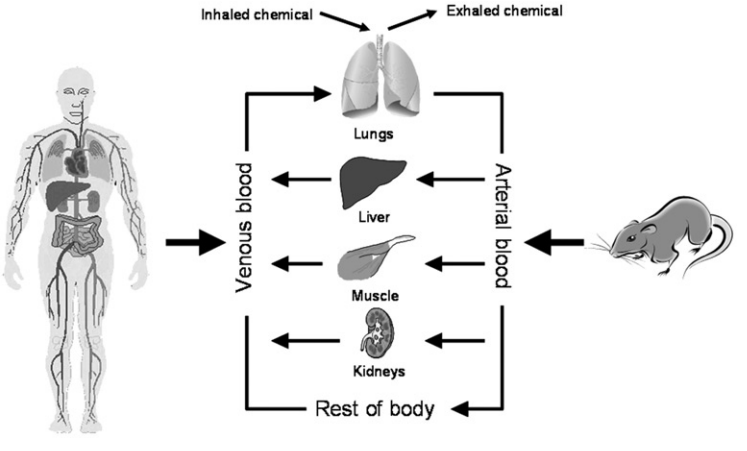

Figure 1. Conceptual representation of a PBPK model for an inhaled toxicant in rats and humans.

velocity (V_{max}) and Michaelis affinity constant (Km) or the intrinsic clearance (V_{max}/Km). The species- and age-specific values of several physiological parameters (Qp, Qc, Qt, Vt) are available in the biomedical and physiology literature [21,25,26]. However, the physicochemical (P_{ba}, P_{ta}, P_{tb}) and biochemical (V_{max}/Km) parameters need to be determined experimentally or predicted using animal-replacement methods for each chemical individually.

Even though *in vivo* and *in vitro* methods for determining blood:air, tissue:air, tissue:blood partition coefficients exist (e.g. equilibrium dialysis, vial equilibration, ultrafiltration, steady-state kinetic studies) [21], they are time- and resource-consuming, particularly for chemicals for which analytical method development has not been achieved. Similarly, the metabolic constants can be determined experimentally *in vivo* using the kinetic data from invasive sampling (parent chemical or metabolite), closed/open chamber,

Downloaded by [Montana State University Bozeman] at 08:07 20 August 2014

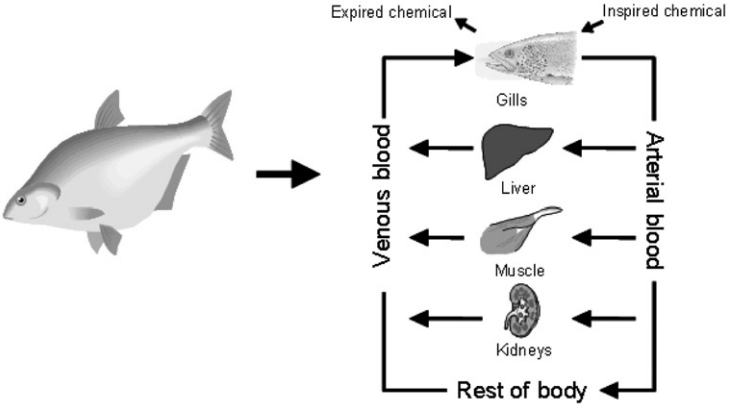

Figure 2. Conceptual representation of a fish PBPK model.

Table 1. Equations used in PBPK models to simulate the pharmacokinetics of inhaled volatile organic chemicals (VOCs) [21].

Compartment	*Input parameters*	*Equations*
Arterial blood	Qc, Qp, P_{ba}, $Cinh$	$Ca = \dfrac{Qc \cdot Cv + Qp \cdot Cinh}{Qc + Qp/P_{ba}}$
Metabolizing tissue (liver)	Ql, V_{max}, Km	$\dfrac{dAl}{dt} = Ql \cdot (Ca - Cvl) - \dfrac{V_{max} \cdot Cvl}{Km + Cvl}$
Non-metabolizing tissues	Qt	$\dfrac{dAt}{dt} = Qt \cdot (Ca - Cvt)$
Venous blood	Qt, Qc	$Cv = \dfrac{\sum Qt \cdot Cvt}{Qc}$

Qc: cardiac output ($L\,h^{-1}$); Qp: alveolar ventilation rate ($L\,h^{-1}$); P_{ba}: blood:air partition coefficient; Ql: blood flow rate to liver ($L\,h^{-1}$); Qt: blood flow rate to tissue t ($L\,h^{-1}$); $Cvl(Cvt)$: concentration of chemical in venous blood leaving liver (tissue) ($mg\,L^{-1}$ or $mmol\,L^{-1}$); Ca: arterial blood concentration ($mg\,L^{-1}$ or $mmol\,L^{-1}$); $Cinh$: inhaled air concentration ($mg\,L^{-1}$ or $mmol\,L^{-1}$); Cv: venous blood concentration ($mg\,L^{-1}$ or $mmol\,L^{-1}$); Al: amount in liver (mg or mmol); V_{max}: Maximal velocity of enzymatic reaction ($mg\,h^{-1}$ or $mmol\,h^{-1}$); Km: Michaelis–Menten affinity constant ($mg\,L^{-1}$ or $mmol\,L^{-1}$).

gas uptake, or exhaled chamber methods; *in vitro* data collected from isolated organ, tissue slices, cells, microsomes, etc. can be used to scale to *in vivo* conditions based on careful considerations of differences in determinants between the *in vitro* and *in vivo* systems [21,27,28]. As the experimental evaluation of the absorption, distribution and clearance parameters for each chemical is time- and resource-consuming, it has led to exploratory work on *in silico* methods for parameterizing PBPK models [29,30].

If SARs, QSARs, QSPRs or QPPRs (referred to hereafter as QSARs) can be developed for predicting the numerical values, or for generating at least some initial estimates or bounds, of the chemical-specific parameters such as P_{ba}, P_{ta}, P_{tb}, $V_{\max}$ and Km, then it will be feasible to make *a priori* predictions of the *in vivo* kinetics of new and untested chemicals. Integration of structure- or property-based algorithms with animal anatomy and physiology information could provide a logical and scientifically-sound means of generating first-cut estimates of the pharmacokinetic behaviour of data-poor chemicals. Basically, in the case of a chemical for which pharmacokinetic parameter database is either incomplete or lacking, the internal dose cannot be reliably estimated (Figure 3A); at the outset, the internal dose measure associated with a particular exposure scenario could vary from anywhere between zero (theoretical minimum) and the potential dose (theoretical maximum). This large uncertainty is due to the fact that there is a lack of precise knowledge regarding the key chemical-specific determinants of ADME (e.g. P_{tb}, P_{ta}, P_{ba}, CL_{int}). Since these parameters, together with the physiology of the animal species, determine the pharmacokinetics (particularly the internal dose) of chemicals in biota, integrated QSAR-PBPK models can effectively predict or identify the possible range of internal dose (Figure 3B). The level of accuracy required for the QSARs then would depend not only upon the intended end-use purpose(s) but also on the sensitivity of the specific input parameters with respect to the model outcome, i.e. predicted internal dose.

This article presents (1) an overview of the QSARs available for predicting the chemical-specific pharmacokinetic determinants, specifically, the partition coefficients (PCs) and metabolic constants, as well as (2) the state-of-the-art for their integration within PBPK models to provide predictions of pharmacokinetics of environmental contaminants in biota.

2. QSARs of PCs for PBPK models

The tissue:plasma PCs along with the volumes of tissues and blood determine the apparent volume in which a chemical is distributed in the exposed organism [31]. On the other hand, the plasma:air or blood:air PC along with the alveolar ventilation rate determines the lung clearance of volatile chemicals [21]. Partition coefficients for PBPK modelling can be predicted following diverse approaches ranging from linear regression to biologically-based algorithms incorporating QSARs [29,30].

Several investigators have explored and established the feasibility of predicting the tissue:blood PCs or the Ostwald solubility from measurements of liposolubility such as P_{ow} and solubility in *n*-octanol or vegetable oil using the linear free energy (LFE) approach [32–48]. The LFE-type QSARs have mainly focused on using steric or hydrophobic descriptors. For example, Abraham et al. [47] developed equations for predicting hydrophobic descriptors (i.e. octanol:water, hexadecane:water, alkane:water and cyclo-hexane:water PCs) based on properties including the McGowan volume, an indicator of

Downloaded by [Montana State University Bozeman] at 08:07 20 August 2014

Downloaded by [Montana State University Bozeman] at 08:07 20 August 2014

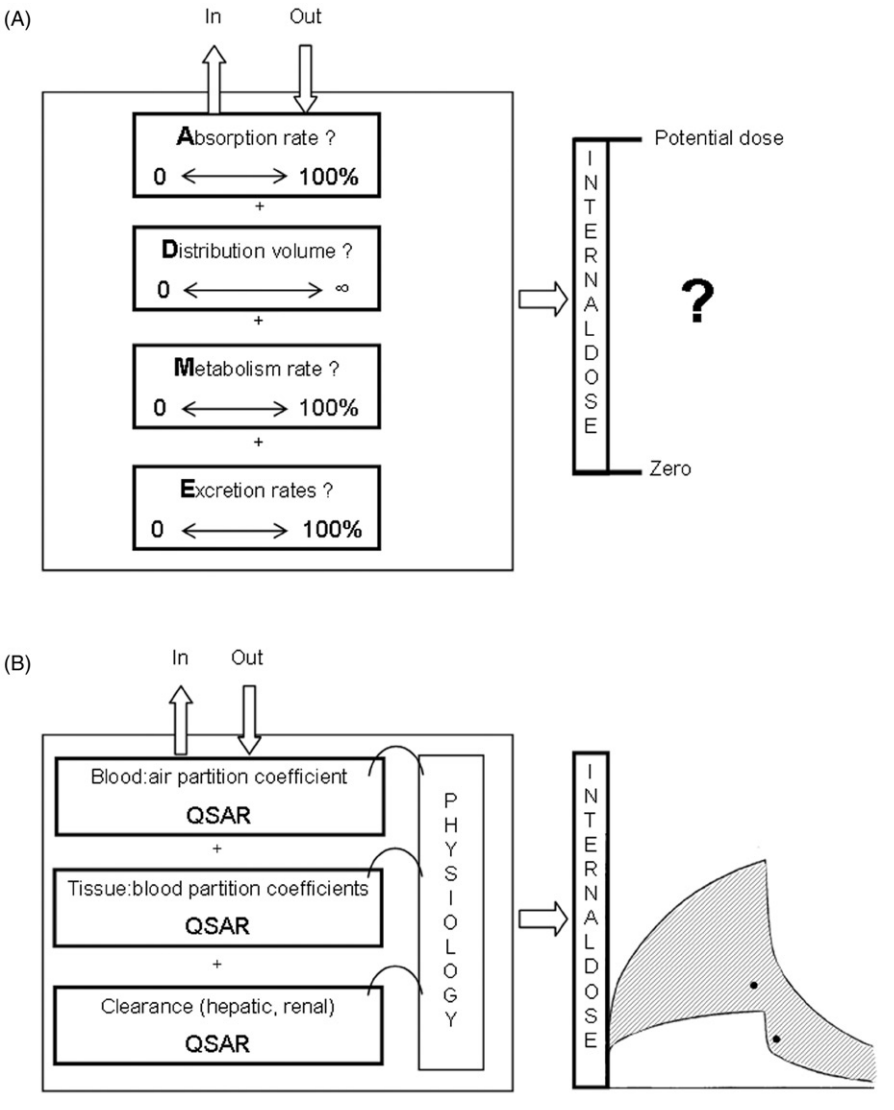

Figure 3. Uncertainty in internal dose calculations for an inhaled toxicant (e.g. target tissue concentration *vs.* time) as a function of the knowledge of pharmacokinetic processes and determinants. (A) A situation characterized by a total lack of experimental or modelled data on pharmacokinetic processes. (B) A situation characterized by the availability of QSAR-based estimates of input parameters and animal physiology, which are integrated within a PBPK modelling framework.

compound bulkiness:

$$\log SP = c + rR_2 + s\pi_2^H + a\alpha_2^H + b\beta_2^H + vV_X \tag{1}$$

$$\log P = 0.088 + 0.562R_2 - 1.054\pi_2^H + 0.034\alpha_2^H - 3.460\beta_2^H + 3.814V_X \tag{2}$$

$$n = 613, \quad r = 0.9974, \quad \text{sd} = 0.116, \quad F = 23161.6$$

where SP is the solute property (e.g. solute octanol:water PC); $\log P$ is the logarithm of n-octanol:water PC; R_2 is the solute excess molar refraction; π_2^H is the solute dipolarity/polarizability; α_2^H is the sum of hydrogen-bond acidity of the solute; β_2^H is the sum of hydrogen-bond basicity of the solute and V_X is the solute McGowan's volume.

Abraham and Weathersby [48] used a multilinear equation combining the solute excess molar refraction, the solute dipolarity/polarizability and the overall hydrogen bond acidity or basicity along with the log hexadecane PC to predict the oil ($n=88$), water ($n=75$), blood ($n=82$), plasma ($n=32$), brain ($n=41$), muscle ($n=41$), lung ($n=36$), liver ($n=29$), kidney ($n=36$), heart ($n=24$), and fat ($n=36$):air PCs for several inorganic and organic chemicals including helium, neon, argon, krypton, xenon, hydrogen, oxygen, nitrogen, nitrous oxide, alkanes, haloalkanes, ketones, alkenes, alcohols and aromatic hydrocarbons:

$$\log L = c + rR_2 + s\pi_2^H + a\alpha_2^H + b\beta_2^H + l\log L^{16} \tag{3}$$

where L is the Ostwald solubility (media:air PC); R_2 is the solute excess molar refraction; π_2^H is the solute dipolarity/polarizability; α_2^H is the sum of hydrogen-bond acidity of the solute; β_2^H is the sum of hydrogen-bond basicity of the solute; and L^{16} is the Ostwald solubility of hexadecane at 298 K.

In this study, the resulting models performed better for water ($n=75$; $r=0.9974$; sd $=0.182$; $F=912.8$) and olive oil ($n=88$; $r=0.9985$; sd $=0.082$; $F=7079.0$), rather than for kidney ($n=36$; $r=0.9753$; sd $=0.266$; $F=117.1$) and heart ($n=24$; $r=0.9784$; sd $=0.172$; $F=117.1$). Abraham and Weathersby [48] observed that non-polar solutes only needed hexadecane:air partitioning (a lipophilic descriptor) to predict the human tissue:air PCs, whereas electrostatic descriptors (i.e. solute dipolarity/polarizability, and hydrogen bond acidity or basicity) were important for functionally substituted compounds such a 1-propanol.

The development of LFE-type QSARs for blood and tissue partitioning was initially based on data for anaesthetic gases [46,49–52]. Since these compounds are relatively lipophilic, the best regression equations were observed for those containing hydrophobic parameters or measures of solubility in lipids and water. Batterman et al. [53] developed quantitative relationships between the human blood:air PCs of four trihalomethanes (chloroform, bromodichloromethane, chlorodibromomethane, and bromoform) and various descriptors including molecular weight and number of bromine atoms in the compound:

$$\log K_{ba} = 0.0072\mathrm{MW} + 0.197 \quad r^2 = 0.994 \tag{4}$$

where K_{ba} is the blood:air PC and MW is the molecular weight;

$$\log K_{ba} = 0.321N + 1.06 \quad r^2 = 0.994 \tag{5}$$

where N is the number of bromine atoms.

Since the above descriptors tend to be correlated with lipophilicity (i.e. increases in molecular weight or number of bromine tend to increase P_{ow}), these types of correlations, especially for such a reduced dataset, are also to be expected. DeJongh et al. [54], Meulenberg and Vijverberg [55] and Meulenberg et al. [56] used the hydrophobic descriptors P_{ow}, P_{oa}, and P_{wa} to relate to rat and human blood:air and tissue:air PCs of VOCs.

Downloaded by [Montana State University Bozeman] at 08:07 20 August 2014

Meulenberg and colleagues [55,56] used the following regression for the tissue:air PCs:

$$P_{ta} = aoP_{oa} + asP_{sa} + c \quad (6)$$

where P_{ta} is the tissue:air PC; P_{oa} is the oil:air PC and P_{sa} is the saline:air PC.

This resulting model exhibited r^2 values of 0.99, 0.92, 0.98, 0.88, 0.99, and 0.98 for blood, fat, brain, liver, muscle, and kidney, respectively. However, contrary to the regression with tissue:air PCs these authors could only derive adequate regressions for blood:air PCs when a significant intercept was included. Since partitioning into lipids and water was taken into account by the hydrophobic descriptors, presence of an intercept was interpreted as being the result of significant binding to blood proteins.

Basak et al. [57] developed QSPRs to predict the human blood:air PCs using principal component regression, partial least squares and ridge regression methods for 31 low-molecular weight VOCs (18 haloalkanes, four haloalkenes, two nitroalkanes, two aliphatic hydrocarbons and five aromatic hydrocarbons) characterized by 221 topostructural (including information on distances; degree complexity; path, cluster, and chain connectivity indices; Wiener index; Balaban's index; triplet indices), topochemical (information theoretic and neighbourhood complexity indices, bond connectivity indices; triplet indices; number of non-hydrogen atoms, number of elements in a molecule; molecular weight; Wiener number; hydrogen bond donor indices, E-state descriptors) and geometrical (Kappa zero, Kappa simple and alpha indices) molecular descriptors. The regression analyses were conducted using one or more (combined) classes of molecular descriptors and with all the chemicals or with only the haloalkanes. In general, the ridge regression that used only the topochemical parameters (i.e. molecular weight, quantifying molecular size, triplet indices, encoding information about the nature of atoms, electrotopological state indices, valence and bonding connectivity indices hydrogen bonding parameter) was found to be superior to the other QSPRs (Q^2 leave-one-out = 0.874; PRESS = 7.79). This study also reported a comparison between the QSPRs and the quantitative property–property relationships (QPPR) based on saline:air along with oil:air PCs or rat blood:air PCs. The QSPRs were found to be comparable or superior to the QPPRs using oil and saline:air PCs; furthermore the rat blood:air PC was shown to be the best predictor of the human blood:air PC. Since the value of rat blood:air PC is not routinely measured, the ridge regression QSPRs were developed to permit the prediction of the human blood:air PC based on quickly calculable molecular descriptors. A similar approach was used by these authors to develop QSPRs for predicting the tissue:air (fat, brain, liver, muscle, kidney) PCs in rats and humans [58]. The QSPRs included topostructural, topochemical, three-dimensional, and *ad initio* quantum chemical molecular descriptors as independent variables for 131 chemicals (alkanes, haloalkanes, nitroalkanes, alcohol, ketones, acetates, ethylenes, cycloalkanes, halogenated and non-halogenated aromatic hydrocarbons). Again, the ridge regression compared to the principal component regression and partial least squares provided the best results and the most significant types of molecular descriptors in the QSPRs were: hydrogen bonding descriptors (number of hydrogen bond donors and acceptor, hydrogen bond donor and acceptor indexes), the polarity descriptor, and the molecular size and shape indices (bond and valence connectivity indexes, number of paths of length of order 1 and 2).

There have been only limited efforts towards the development and evaluation of QSARs for computing PCs of non-volatile, environmental chemicals. In this regard, Parham et al. [59] developed QSARs using steric descriptors, for estimating adipose

Downloaded by [Montana State University Bozeman] at 08:07 20 August 2014

tissue:plasma and adipose tissue:blood PCs of a congeneric series of 24 polychlorinated biphenyls (PCBs) (from bichlorophenyl to octachlorophenyl). The descriptors included in the model reflected aspects such as the planarity, the number and position of chlorines, as well as the effect of the chlorines on the adjacent carbons. After a stepwise analysis, the following QSPR ($r^2 = 0.77$) for the logarithm of the adipose tissue:plasma PC ($\log K_{fp}$) was obtained:

$$\log K_{fp} = 1.9988 - 0.5004\ \mathrm{UNS} + 0.1793\ \mathrm{NPL} + 0.05931\ \mathrm{DIFF}^2 \tag{7}$$

where UNS = 1 if the number of adjacent non-chlorine-substituted *ortho-meta* carbon pairs is higher than 0, UNS = 0 otherwise; NPL is the non-planarity index, equal to the number of ortho (2,6,2′, or 6′) chlorines if the number is less than 2, otherwise equal to 2; and DIFF is the difference between the number of chlorines on the most-substituted ring and the number of chlorines on the least-substituted ring (measure of polarity).

The fat:blood PC was in turn calculated based on the fat:plasma PC and the fraction of PCBs in the blood cells (f_{cr}), which in turn was calculated using the following QSPR ($r^2 = 0.94$):

$$f_{cr} = 0.1954(\pm 0.0586) + 0.1513(\pm 0.0352)\mathrm{NUNMP} \tag{8}$$

where NUNMP is the number of adjacent non-chlorine-substituted *ortho-meta* carbon pairs.

It was shown that the PCs depended mostly on the presence or absence of adjacent non-chlorine-substituted *meta* and *para* carbons. Since PCB congeners without unsubstituted *meta-para* pairs tended to be more slowly eliminated than those with such pairs, it was suggested that the reason for this slower elimination might be the higher adipose tissue:blood PC, leading to a greater storage of PCBs in this tissue [59].

Gargas et al. [60] used connectivity indexes and *ad hoc* descriptors in order to correlate structure with the rat tissue:air PCs of a series of 25 haloalkanes (methanes, ethanes, ethylenes with log olive oil:water PC values between 0.56 and 3.43). The following QSARs for the fat:air PC, based on higher order connectivity indices and ad hoc descriptors (Q_H: polar hydrogen factor; N_{Cl}, N_{Br}, N_C, N_F: number of chlorine, bromine, carbon, and fluorine atoms, respectively) were obtained in this study:

$$\begin{aligned}\log P_{fa} = {} & 0.734(\pm 0.096)^1\chi^v - 0.029(\pm 0.003)\left(\chi_s^v\right) - 1.570(\pm 0.284)\left(1/^1\chi\right) \\ & - 0.559(\pm 0.167)\left(1/^1\chi^v\right) - 0.098(\pm 0.038)^3\chi_c^{v^v} + 2.213(\pm 0.365) \\ r^2 = {} & 0.9779, \quad s = 0.1348\end{aligned} \tag{9}$$

$$\begin{aligned}\log P_{fa} = {} & 0.563(\pm 0.028)N_{Cl} + 1.028(\pm 0.065)N_{Br} + 0.467(\pm 0.060)N_C \\ & + 0.270(\pm 0.036)Q_H - 0.199(\pm 0.034)N_F - 0.097(\pm 0.121) \\ r^2 = {} & 0.9781, \quad s = 0.1341\end{aligned} \tag{10}$$

These authors reported that fluorine substitution reduced the tissue solubility, with the greatest effect being observed in biological matrices with the greatest volume fraction of water (e.g. blood). On the contrary, the chlorine and bromide substituents increased solubility in all tissues. Because of the electronegativity of these atoms (F < Cl < Br), it was suggested that these atoms increased the solubility in the media via dispersion interactions. Their study results indicate that it is challenging to evaluate the 'steric'

Downloaded by [Montana State University Bozeman] at 08:07 20 August 2014

Downloaded by [Montana State University Bozeman] at 08:07 20 August 2014

influence independent of the 'hydrophobic' influence, as they relate to tissue solubility of environmental chemicals [60]. More recent work focused on evaluating the contribution of each molecular fragment to the tissue and blood partitioning processes in a global manner. Accordingly, the Free–Wilson approach was used, reflecting the working hypothesis that each substituent in the molecular structure had an additive and constant contribution to the PC of interest [61]:

$$PC = \sum_{i=1}^{n} Cf_i \cdot f_i \tag{11}$$

where Cf_i is the contribution of the fragment i to the value of the PC and f_i corresponds to the frequency of occurrence of the fragment in the molecule.

Using the above approach, Béliveau et al. [62] carried out linear regression analysis based on the frequency of occurrence of 11 different structural fragments (CH_3, CH_2, CH, C, C=C, H, Cl, F, Br, benzene ring (AC) and H in benzene ring (H on AC)) and the logarithm of published data on tissue:air and blood:air PCs. The experimental data corresponded to the blood:air, fat:air, muscle:air and liver:air PCs of 46 low molecular weight VOCs (16 chloroalkanes, five alkanes, five chloroethylenes, five aromatic hydrocarbons, four bromoalkanes, three bromochloroalkanes, three bromochloroalkanes, two chlorofluoroalkanes, difluoromethane, 2-bromo-2-chloro-1,1,1-trifluoroethane, vinyl bromide, chlorobenzene, allyl chloride and isoprene). All the chemicals were described using combinations of the eleven molecular fragments listed above. Table 2 summarizes the contributions of the molecular fragments to rat blood:air, liver:air, muscle:air and fat:air PCs of low molecular weight VOCs, as determined by Béliveau et al. [62]. These QSPRs were developed using data for alkanes, haloalkanes, haloethylenes, and aromatic hydrocarbons with $\log P$ ranging between 0.56 and 5.44. Some classes of haloalkanes, particularly the fluorinated hydrocarbons, were poorly represented in the calibration dataset and thus the predictions of the log PCs using the group contribution represented in Table 2 can have large uncertainty for such chemicals. However, the chlorinated

Table 2. Fragment contribution to rat partition coefficients.[a]

	Fragment contribution to			
Fragment	*Blood:air*	*Liver:air*	*Muscle:air*	*Fat:air*
CH_3	0.072	0.016	−0.020	0.366
CH_2	0.109	0.234	0.122	0.435
CH	0.079	0.359	0.266	0.330
C	−0.606	0.032	−0.105	−0.285
C=C	−0.494	0.257	−0.707	0.327
H	0.236	−0.031	0.081	0.155
Br	0.834	0.700	0.622	1.170
Cl	0.481	0.384	0.322	0.735
F	0.020	−0.113	−0.911	0.075
AC	2.850	3.760	3.650	2.920
H on AC	−0.292	−0.408	−0.446	−0.056

[a]AC: benzene ring; the fragment contributions times the frequency of their occurrence gives the logarithm of the particular partition coefficient. Based on Béliveau et al. [62].

hydrocarbons are well represented in the dataset; therefore the QSPR model may be more adequate for application to this sub-class of VOCs. Based on these data, for example, the predicted logarithm of the blood:air PC of the 1,2-dichlorethane would equal: $(2 \times 0.481) + (2 \times 0.109) = 1.18$.

Using a similar methodology, Kamgang et al. [63] developed QSPRs for predicting fat:air and blood:air PCs of VOCs. The linear regression analysis was conducted with published *in vitro* data of fat:air and blood:air PCs for 20 non-halogenated VOCs (alkanes, alkenes and aromatic hydrocarbons). The eight fragments used in the regression were the same as those listed in Table 2 (i.e. without the three halogens). Table 3 summarizes the fragment contributions to the rat blood:air PCs and the fat:air PCs, as obtained by these authors. Interestingly, the group contributions that were significant in the analysis of Kamgang et al. [63] (CH_2, H, AC H on AC for blood:air PC; and CH_3, CH_2, CH, H, AC for fat:air PC) were comparable to those reported by Béliveau et al. [62] (Table 2).

Contributions of individual fragments to the model parameters are expected to be dependent on the tissue composition of the species of interest and would vary from one species to another. Accordingly then, several Free–Wilson type QSARs would be required for computing the PCs in multiple tissues and species [62–64]. Should the nature and concentrations of lipids, proteins and water be the same in two tissues of the species of interest, then the calculated molecular fragment contributions are expected to be identical in these species. Ideally then, the strategy would be to incorporate species-specific differences in tissue composition along with chemical-specific parameters reflective of liposolubility. In this regard, a number of tissue composition-based algorithms are potentially of particular use.

The mechanistic, tissue composition-based algorithms for predicting PCs for PBPK modelling were developed by considering ionization, solubility and binding in the various matrices (i.e. intracellular, interstitial, vascular) [65–79]. The fundamental principle of these mechanistic algorithms is that the concentration (or solubility) of a chemical in a biological matrix can be expressed as the sum of its concentration in the key components of the matrix (i.e. water, neutral lipids, charged phospholipids, haemoglobin and/or

Table 3. Fragment contributions to rat fat:air and blood:air PCs.[a]

	Fragment contribution to	
Fragment	*Blood:air*	*Fat:air*
CH3	−0.024	0.277
CH2	0.105	0.369
CH	0.186	0.395
C	0.129	0.276
H	0.065	0.267
AC	2.747	3.295
H on AC	−0.252	−0.120

AC: benzene ring.
[a]The group contributions times the frequency of their occurrence gives the logarithm of the particular partition coefficient. Based on Kamgang et al. [63].

Downloaded by [Montana State University Bozeman] at 08:07 20 August 2014

plasma proteins). Accordingly, for environmental chemicals, the tissue:air PCs have been computed as follows [72]:

$$P_{ta} = P_{oa} \cdot F_{nlt} + P_{wa} \cdot F_{wt} \quad (12)$$

where P_{ta} is the tissue:air PC; P_{oa} is the olive oil:air PC; F_{nlt} is the fractional content of neutral lipids equivalent in tissue; P_{wa} is the water:air PC; and F_{wt} is the fractional content of water equivalent in tissue.

Equation (12) for predicting matrix:air PC are adequate only for VOCs that do not bind significantly to macromolecules. For chemicals that bind significantly to biological macromolecules in blood or tissues, the bound concentrations should be taken into account in computing the apparent PCs [71,80]. In such cases, the prediction of PCs from molecular structure information is compounded by the difficulty of predicting the binding association constants. Béliveau et al. [81], based in the work of Poulin and Krishnan [71], used the following equation to calculate the blood:air PC:

$$P_{ba} = P_{oa} \cdot (F_{nlb} + 0.3 \cdot F_{plb}) + P_{wa} \cdot (F_{wb} + 0.7 \cdot F_{plb}) + f_b \cdot P_{pa} \cdot F_{pb} \quad (13)$$

where P_{oa} is the *n*-octanol:air or oil:air PC predicted from molecular structure information; P_{wa} is the water:air PCs predicted with molecular structure information; P_{pa} is the protein:air PCs predicted with molecular structure information; F_{nlb} is the fraction of neutral lipids in blood; F_{plb} is the fraction of phospholipids in blood; F_{wb} is the fraction of water in blood; F_{pb} is the fraction of proteins in blood and f_b is the fraction of proteins involved in binding.

In the above algorithms, the solubility of the chemical in blood and tissue is described as the sum of its solubility in neutral lipids, phospholipids and water. Here, the phospholipids are assumed to behave as a mixture of neutral lipids (30%) and water (70%), based on literature evidence of the hydrophobicity characteristics of commercial lecithin [70]. According to this approach, the numerical values of P_{ba} and P_{ta} can be predicted with knowledge of (1) blood and tissue lipid, water and protein levels (F_{nlb}, F_{nlt}, F_{plb}, F_{plt}, F_{wb}, F_{wt} and F_{pb}) and (2) the numerical values of P_{oa}, P_{wa} and P_{pa}. Species-specific data on the levels of lipids, water and proteins are available in the literature [42,69,70,73,81–83] (e.g. Table 4). Once the numerical values of these species-specific parameters are included in the above equations, P_{ta} and P_{ba} can be predicted solely from

Table 4. Fractional content of the key components in blood and tissues of rats and humans.

Species	*Component*[a]	*Blood*	*Fat*	*Liver*	*Muscle*
Rat	Neutral lipids	0.002	0.8536	0.0425	0.0117
	Water	0.8423	0.1215	0.7176	0.7471
	Proteins	0.156	–	–	–
Human	Neutral lipids	0.004	0.7986	0.0473	0.0378
	Water	0.8217	0.1514	0.74	0.7573
	Proteins	0.174	–	–	–

[a]'Neutral lipids' represent the sum of neutral lipid content and 30% of phospholipids in the biological matrix. 'Water' represents the sum of water content and 70% of phospholipids in the biological matrix. Based on data compiled/reported by Poulin and Krishnan [69,70], Béliveau et al. [81] and Krishnan and Peyret [82].

Downloaded by [Montana State University Bozeman] at 08:07 20 August 2014

knowledge of P_{wa} and P_{oa} (and additionally P_{pa} in the case of rat). Here, P_{oa}, the *n*-octanol:air or oil:air partition coefficient, is reflective of the chemical partitioning into the tissue lipids whereas the tissue water:air PC is considered to be the same as the inverse of the Henry's law constant.

Thus, the tissue composition-based algorithms account for both physiological and physicochemical characteristics. For example, in the algorithms for predicting tissue:air and blood:air PCs (Equations (12) and (13)), the physiological input parameters correspond to the composition of the tissue or the blood, whereas the physicochemical parameters are the oil:air PC, the water:air PC and, additionally, protein:air PC for the blood:air PC [71,72,81]. QSARs for predicting oil:air (or *n*-octanol:air), water:air and blood protein:air PCs are available in the literature [35,81,84–86], facilitating the computation of PCs for different species for the purpose of PBPK modelling. In this regard, Béliveau et al. [81] developed QSPRs for oil, water, and protein:air PCs, and then integrated the results with the tissue and blood composition data for rats and humans to predict the tissue:air (i.e. muscle, liver, and fat), and blood:air PCs, as per Equations (12) and (13). Table 5 summarizes the findings of this QSPR analysis, specifically the contributions of the fragments to the numerical values of olive oil:air, water:air and protein:air PCs, for computing tissue and blood:air PCs. These fragment contributions and QSARs are not specific to any species because they are only used to predict the chemical-specific input parameters of the algorithm. In turn, upon inclusion of the tissue and blood composition data specific to the species (Table 4), predictions of PCs for various tissues and species become feasible – solely from the molecular structure information.

The mechanistic algorithms for predicting PCs have evolved over the years. Tables 6 and 7 summarize the input parameters and the characteristics of the compounds underlying the development of these algorithms. Most of the refinements of the PC algorithms as well as QSARs for binding to albumin have been accomplished based on data for pharmaceutical substances [65,74–76,87–97]. These advances would potentially be informative for guiding further development of QSARs for PCs of metabolites and other

Table 5. Fragment contributions to oil:air, water:air and protein:air PC[a].

	Fragment contribution to		
Fragment	*Oil:air*	*Water:air*	*Protein:air*
CH_3	0.354	−0.038	0.306
CH_2	0.441	−0.223	0.182
CH	0.377	−0.477	−0.111
C	−0.354	−1.490	−1.060
C=C	0.197	−1.940	−0.877
H	0.134	0.555	0.492
Br	1.174	0.622	1.150
Cl	0.776	0.468	0.764
F	0.136	0.229	0.241
AC	3.729	0.650	1.970
H on AC	−0.190	−0.062	−0.028

[a]AC: benzene ring; the fragment contributions times the frequency of their occurrence gives the logarithm of the particular partition coefficient. Based on Béliveau et al. [81].

Downloaded by [Montana State University Bozeman] at 08:07 20 August 2014

Downloaded by [Montana State University Bozeman] at 08:07 20 August 2014

Table 6. Mechanistic algorithms for predicting partition coefficients for PBPK models.

Reference	*Equation*	*Definition of the parameters*	*Comments*
[91]	$K_{pfu} - \frac{1}{fui} = \alpha \cdot P^{\beta}$	K_{pfu}: tissue: unbound plasma; *fui*: non-ionized fraction of the interstitial space; *P*: solvent:water PC (i.e., *n*-octanol, benzene, chloroform and trioleine: water PC)	*n*-octanol:water PC was found to be the best descriptor of the K_{pfu}; *r* values range from 0.96 for bone to 0.987 for brain
[42]	$P_{mw} = 10^{\log P_{ow}} \times F_{nlm} + 1 \times F_{wm}$	P_{mw}: media (blood or tissue):water PC; P_{ow}: *n*-octanol:water PC; F_{nlm}: fraction of non-polar lipids in the media; F_{wm}: fraction of water in the media	The prediction/experimental data of PCs were 2.28 ± 2.27 for blood:water, 1.34 ± 0.81 for fat:blood 0.91 ± 0.38 for kidney:blood, 0.73 ± 0.09 for liver:blood, and 1.2 ± 0.44 for white muscle:blood PCs ($n = 3$). Poor predictions for hexachloroethane blood:water PC (298.23 predicted *vs.* 61.36 measured)
[70]	$P_{tb} = \frac{(S_o \cdot f_{nlt}) + (S_w \cdot 0.7 \cdot f_{plt}) + (S_o \cdot 0.3 \cdot f_{plt}) + (S_w \cdot f_{wt})}{(S_o \cdot f_{nlb}) + (S_w \cdot 0.7 \cdot f_{plb}) + (S_o \cdot 0.3 \cdot f_{plb}) + (S_w \cdot f_{wb})}$	P_{tb}: tissue:blood PC; S_o: solubility in *n*-octanol; S_w: solubility in water; f_{nl}: fraction of neutral lipids; f_{pl}: fraction of phospholipids; f_w: fraction of water; *t*: tissue; *b*: blood	For all the tissues studied the predictions were higher than the experimental values, but within a factor of 1.48 ($n = 127$). The partition coefficients for which more than one value was reported in the literature, the predicted/experimental ratio was 1.83. ($r = 0.96$)

(*Continued*)

Downloaded by [Montana State University Bozeman] at 08:07 20 August 2014

Table 6. Continued.

Reference	*Equation*	*Definition of the parameters*	*Comments*
[69]	$P_{tb} = \dfrac{P_t}{0.37 \cdot P_e + 0.67 \cdot P_p}$ $P_t = (P_{ow} \cdot f_{nlt}) + (1 \cdot 0.7 \cdot f_{plt}) + (P_{ow} \cdot 0.3 \cdot f_{plt}) + (1 \cdot f_{wt})$ $P_e = (P_{ow} \cdot f_{nle}) + (1 \cdot 0.7 \cdot f_{ple}) + (P_{ow} \cdot 0.3 \cdot f_{ple}) + (1 \cdot f_{we})$ $P_p = (P_{ow} \cdot f_{nlp}) + (1 \cdot 0.7 \cdot f_{plp}) + (P_{ow} \cdot 0.3 \cdot f_{plp}) + (1 \cdot f_{wp})$	P_{tb}: tissue:blood PC; P_t: tissue:water PC; P_p: plasma:water PC; P_e: erythrocyte:water PC; P_{ow}: *n*-octanol (or oil): water PC; f_{nl}: fraction of neutral lipids; f_{pl}: fraction of phospholipids; f_w: fraction of water; *t*: tissue; *e*: erythrocyte; *p*: plasma	Using P_{ow} the predicted/experimental ratio of rat tissue:blood PC was 1.01 ± 0.27 for the muscle and 0.99 ± 0.35 for the liver ($n = 21$). The predictions of the fat:blood PC were found to be better when using the vegetable oil:water PC as input parameter, rather than the P_{ow} (1.5 ± 0.74; $n = 21$)
[72]	$P_{ta} = P_{oa} \cdot f_{nlt} + P_{wa} \cdot 0.7 \cdot f_{plt} + P_{oa} \cdot 0.3 \cdot f_{plt} + P_{wa} \cdot f_{wt}$	P_{ta}: tissue:air PC; P_{oa}: *n*-octanol:air PC; P_{wa}: water:air PC; f_{nl}: fraction of neutral lipids; f_{pl}: fraction of phospholipids; f_w: fraction of water; *t*: tissue; *e*: erythrocyte; *p*: plasma	The predicted/experimental ratio of tissue:air PC was 0.94 ± 0.38 ($n = 45$) for liver, 0.93 ± 0.46 ($n = 45$) for muscle, and 1.1 ± 0.35 ($n = 45$) for fat.
[71]	$P_{ba,app} = P_{ba} + \left(1 + \dfrac{Ka \cdot C_p}{(1 + Ka \cdot Ca_{free})}\right)$ $P_{ba} = P_{oa} \cdot f_{nlb} + P_{wa} \cdot 0.7 \cdot f_{plb} + P_{oa} \cdot 0.3 \cdot f_{plb} + P_{wa} \cdot f_{wb}$	$P_{ba,app}$: apparent blood:air PC; P_{ba}: solubility-based predicted blood:air PC; *Ka*: affinity for hemoglobin; C_p: concentration of haemoglobin in blood Ca_{free}: concentration of the free form of the compound in the erythrocyte	The blood:air PC of the hydrophilic compounds was well predicted without considering the protein binding (i.e. using P_{ba}) (predicted/experimental ratio $= 0.80 \pm 0.21$; $n = 18$); the hydrophobic VOCs could not be adequately predicted without this mechanism (predicted/experimental ratio $= 0.21 \pm 0.07$; $n = 27$).

Downloaded by [Montana State University Bozeman] at 08:07 20 August 2014

[54]	$PC_{tb} = \frac{V_{lt} \times K_{l:wt} + V_{w,t}}{V_{lb} \times K_{l:wb} + V_{wb}} + B$	V_l: volume of lipids; V_w: volume of water t: tissue; b: blood; $K_{l:wt}$: lipid:water PC in tissue; $K_{l:wb}$: lipid:water PC in blood; B: empirical constant	The $K_{l:wt}$ were calculated from octanol:water PC. $K_{l:wb}$ and B were fitted to the PC data. The predictions of this algorithm were more accurate with the human data than in rats. The term B may account for chemical-specific binding to proteins. $r^2 = 0.99$ (liver) to 1 (other tissues) for human PCs, and $r^2 = 0.24$ (muscle), 0.58 (liver), 0.98 (fat) for rat PCs. For most chemicals, the predicted/experimental ratios were 0.5–2.
[66]	$P_{fb} = \frac{F_{nef}}{F_{neb}}$	P_{fb}: fat:blood PC; F_{nef}: fractional content of neutral lipids equivalent in fat; F_{neb}: fractional content of neutral lipids equivalent in blood	For highly hydrophobic compounds (i.e. with $\log P > 6$), the predicted tissue:blood PC is a constant, but species-specific.
[89]	$P_{tp} = f_{wt} \cdot \left\lfloor 1 + \theta_{1t} \cdot 10^{\theta_{2t} \log P_{ow}} \right\rfloor$	P_{tp}: tissue:unbound plasma PC; f_{wt}: fractional content of water in tissue; θ_1 and θ_2: empirical terms; P_{ow}: n-octanol:water PC	θ_1 and θ_2 fitted to data. Mean prediction error (ME) between −22.48 and 61.14%. Square root of the mean square prediction error (RMSE) between 28.33 and 85.2%.
[87]	$\log P_{tb} = \log \frac{\left(\alpha \cdot \frac{f_{mt}}{f_{wt}} + \gamma \cdot \frac{f_{pt}}{f_{wt}}\right) \cdot P_{ow}^{\beta_t} + 1}{\left(\alpha \cdot \frac{f_{mb}}{f_{wb}} + \gamma \cdot \frac{f_{pb}}{f_{wb}}\right) \cdot P_{ow}^{\beta_b} + 1} + \log \frac{f_{wt}}{f_{wb}}$	P_{tb}: tissue:blood PC; $\alpha \cdot P^{\beta}$: membrane:water PC; $\gamma \cdot P^{\beta}$: association constant to proteins (Ka_{pr}); f : fractional content;	α and γ are chemical specific whereas β is more specific to the tissue. α, γ and β were fitted to experimental data. Worst fit for heart PCs

(*Continued*)

Downloaded by [Montana State University Bozeman] at 08:07 20 August 2014

Table 6. Continued.

Reference	*Equation*	*Definition of the parameters*	*Comments*
		t: tissue; b: blood; m: membrane; w: water ; p: protein;	($n=14$; $r=0.837$; $s=0.080$; $F=28.1$), and best fit for fat PCs ($n=36$; $r=0.98$; $s=0.198$; $F=188$)
[81]	$P_{ba} = P_{oa} \cdot f_{nle} + P_{wa} \cdot f_{we} + fb \cdot f_p \cdot P_{pa}$	P_{ba}: blood:air PC; P_{oa}: oil:air PC; P_{wa}: water:air PC; P_{pa}: protein:air PC; f_{nle}: fraction of neutral lipid equivalent in blood; f_{we}: fraction of water equivalent in blood; f_p: fraction of proteins in blood; fb: fraction of total proteins involved in the partitioning	QSPRs were developed for P_{oa}, P_{wa}, and P_{pa}. The predicted/experimental ratio was 0.87 ± 0.44 (range: 0.21–1.88) in humans and 1.10 ± 0.53 (range: 0.24–2.69) in rats.
[65]	$P_{tp} = \frac{P_{vow} \cdot (V_{nlt} + 0.3 \cdot V_{plt}) + 1 \cdot (V_{wt} + 0.7 \cdot V_{plt})}{P_{vow} \cdot (V_{nlp} + 0.3 \cdot V_{plP}) + 1 \cdot (V_{wp} + 0.7 \cdot V_{plp})} \cdot \frac{fu_p}{fu_t}$	P_{tp}: tissue:plasma PC; P_{vow}: oil:water PC; V_{nl}: volume of neutral lipids; V_{pl}: volume of phospholipids; V_w: volume of water; t: tissue; p: plasma	For all tissues and species studied predicted/experimental ratio was 1.26 ± 1.40 ($n=269$)
[90]	$P_{fp} = \frac{P_{vow} \cdot (V_{nlf} + 0.3 \cdot V_{plf}) + 1 \cdot (V_{wf} + 0.7 \cdot V_{plf})}{P_{vow} \cdot (V_{nlp} + 0.3 \cdot V_{plp}) + 1 \cdot (V_{wp} + 0.7 \cdot V_{plp})} \cdot \frac{fu_p}{1}$	P_{tp}: fat:plasma PC; V_{nl}: volume of neutral lipids; V_{pl}: volume of phospholipids; V_w: volume of water; f: fat; p: plasma	Overall predicted/experimental ratio was 1.17 ± 0.44 ($n=14$) using P_{vow} corrected for the ionization

Downloaded by [Montana State University Bozeman] at 08:07 20 August 2014

[88]	$P_{tp} = \frac{P_{vow} \cdot (f_{nlt} + 0.3 \cdot f_{plt}) + 0.7 \cdot f_{plt} + f_{wt}/fu_t}{P_{vow} \cdot (f_{nlp} + 0.3 \cdot f_{plp}) + 0.7 \cdot f_{plp} + f_{wp}/fu_p}$	P_{tp}: tissue:plasma PC P_{vow}: oil:water PC; f_{nl}: fraction of neutral lipids; f_{pl}: fraction of phospholipids; f_w: fraction of water; t: tissue; p: plasma	Suggested correction of the algorithm of Poulin and Theil, considering that there are no macromolecules to interact within phospholipids
[75]	$Kpu = f_{EW} + \frac{X \cdot f_{IW}}{Y} + \frac{P_{ow} \cdot F_{NL} + (0.3 \cdot P_{ow} + 0.7) \cdot f_{NP}}{Y} + Ka_{PR} \cdot [PR]_T$	Kpu: tissue:unbound plasma PC; P_{ow}: n-octanol (or oil for adipose tissue):water PC; f_{EW}: fraction of extracellular water in the tissue; f_{IW}: fraction of intracellular water in the tissue; f_{NL}: fraction of neutral lipids in the tissue; f_{NP}: fraction of neutral phospholipids in the tissue; Ka_{PR}: association constant to proteins; $[PR]_T$: concentration of plasma proteins in the tissue; X and Y are ionization correction terms for the intracellular and plasma water, respectively	Ka_{PR} derived from fraction unbound in plasma. Using experimental values of P_{ow} and pKa the predicted/experimental ratio was 1.62 ± 2.17 for acids, 1.09 ± 1.32 very weak bases, and 0.91 ± 0.79 for all the studied drugs

(*Continued*)

Downloaded by [Montana State University Bozeman] at 08:07 20 August 2014

Table 6. Continued.

Reference	*Equation*	*Definition of the parameters*	*Comments*
[77–79]	$\log PC = \log\left(10^{\log Fl+\log Plb} + 10^{\log Fp+\log Ppb} + 10^{\log Fw+\log Pwb}\right)$	*PC:* tissue:blood PC; *Fl*: fraction of lipids; *Fw*: fraction of water; *Fp*: fraction of proteins; *Plb*: lipid:blood PC; *Ppb*: protein:blood PC;; *Pwb*: water:blood PC	QSARs were developed to predict *Plb*, *Ppb* and *Pwb* of neutral ($n=166$, $r^2=0.851$, $s=0.260$, $Q^2=0.833$) [77], neutral and ionized ($n=201$, $r^2=0.905$, $s=0.291$, $Q^2=0.890$) [78] and diverse compounds ($n=248$, $r^2=0.877$, $s=0.352$) [79]
[74]	$Kpu = f_{EW} + \frac{1+10^{pKa-pHiw}}{1+10^{pKa-pHp}} \cdot f_{IW} + \frac{Ka \cdot [AP^-]_T \cdot 10^{pKa-pHiw}}{1+10^{pKa-pHp}} + \frac{P_{ow} \cdot f_{NL} + (0.3 \cdot P_{ow} + 0.7) \cdot f_{NP}}{1+10^{pKa-pHp}}$	*Kpu*: tissue:unbound plasma PC; P_{ow}: *n*-octanol (or oil for adipose tissue):water PC; f_{EW}: fraction of extracellular water in the tissue; f_{IW}: fraction of intracellular water in the tissue; f_{NL}: fraction of neutral lipids in the tissue; f_{NP}: fraction of neutral phospholipids in the tissue; Ka: association constant for	*Ka* derived from erythrocyte:water PC. Overall predicted/experimental ratio was 1.27 ± 1.3

Downloaded by [Montana State University Bozeman] at 08:07 20 August 2014

		acidic phsopholipids; $[AP^-]_T$: acidic phospholipids content in the tissue	
[76]	$K_{tp} = \left(\frac{F_{\text{int}}}{fu_{\text{int}}} + K_{cell:plasma} \cdot \frac{F_{cell}}{fu_{cell}}\right) \cdot fup \times \frac{1}{fu_{\text{int}}} = F_{W\text{int}} + \frac{F_{p\text{int}}}{F_{pp}} \cdot \left(\frac{1}{fu_p} - F_{Wpl}\right) \times \frac{1}{fu_{cell}} = F_W + K_{NL} \cdot F_{NL} + K_{NP} \cdot F_{NP} + K_{APL} \cdot F_{APL} + K_P \cdot F_P$	K_{tp}: tissue:plasma fu_{int}: unbound fraction in interstitium; fu_{cell}: unbound fraction in cellular space; fu_p: unbound fraction in plasma; p: plasma; int: interstitium; F_W, water fraction; F_{NL}: neutral lipid fraction; F_{NP}: neutral phospholipids fraction; F_{APL}: acidic phospholipids fraction; F_p: protein fraction K_{NL}: neutral lipids:water PC; K_{NP}: neutral phospholipids:water PC; K_{APL}: acidic phospholipids:water PC; K_p: intracellular protein:water PC	Equations to calculate K_{NP}, K_{APL}, and K_p from P_{ow} were reported in the original article. 73% of the predictions were within a factor of 3 compared with the experimental values

Downloaded by [Montana State University Bozeman] at 08:07 20 August 2014

Table 7. Algorithms for predicting partition coefficients for PBPK modelling.

Reference	*Partition coefficient*	*Tissues or media*	*Species*	*Compounds studied*	
				Class	*log P_{ow}*
[91]	Tissue:plasma unbound	Lungs, brain, heart, intestine, muscle, fat, skin and bone	Rabbit	Drugs	2.21 to 5.19
[42]	Tissue:water	Muscle	Rainbow trout	Ethanes	2.39 to 4.14
[70]	Tissue:blood	Muscle, brain, adipose tissue, liver, lung, kidney	Human	Alcohols, aromatic hydrocarbons, alkanes, halogenated alkanes, acetone, diethyl ether	−0.82 to 4.83
[69]	Tissue:blood	Liver, muscle, adipose tissue	Rat	Alcohols, ketones, acetate esters, diethyl ether	−0.77 to 2.13
[72]	Tissue:air	Liver, muscle, adipose tissue	Rat	Alcohols, aromatic hydrocarbons, alkanes, halogenated alkanes, acetone, diethyl ether	−0.77 to 3.44
[71]	Blood:air	Blood	Rat	Alcohols, aromatic hydrocarbons, alkanes, halogenated alkanes, acetone, diethyl ether	−0.77 to 3.44
[54]	Tissue:blood	Liver, muscle, fat, kidney and brain	Rat, human	aromatic hydrocarbons, alkanes, halogenated alkanes	0.2 to 4.66
[66]	Tissue:blood	Adipose tissue	Rat, human	Highly lipophilic compounds, PCBs, dioxins	>4
[89]	Tissue:unbound plasma	Lungs, liver, kidneys, stomach, pancreas, spleen, intestine, muscle, fat, skin, bones, heart, brain, testes, erythrocytes	Rat	Barbituric acids	0.11 to 4.04
[87]	Tissue:blood	Fat, liver, brain, kidneys, muscle, lung, and heart	Human	Alcohols, ethers, alkanes, halogenated, alkanes	−2 to 5

Downloaded by [Montana State University Bozeman] at 08:07 20 August 2014

[81]	Blood:air	Blood	Rat, human	Aromatic hydrocarbons, alkanes, halogenated alkanes	0.71 to 4.05
[65]	Tissue:plasma	Brain, heart, lung, muscle, skin, intestine, spleen, bone	Rabbit, rat, mouse	Drugs	−4.62 to 6.28
[90]	Tissue:plasma	Adipose tissue	Rabbit, rat, human	Drugs	0.04 to 4.8
[88]	Tissue:plasma	–	–	–	–
[75]	Tissue:unbound plasma	Adipose tissue, bone, brain, intestine, heart, kidney, liver, lung, muscle, pancreas, skin, spleen, thymus	Rat	Drugs	−1.2 to 4.1
[77]	Tissue:blood	Adipose tissue, liver, brain, kidney, muscle, lung, heart	Human	Alcohols, alkanes, ethers, fluorated ethers, alkenes, aromatic hydrocarbons	−0.77 to 4.66
[78]	Tissue:blood	Adipose tissue, liver, brain, kidney, muscle, lung, heart	Human	Alcohols, alkanes, ethers, fluorated ethers, alkenes, aromatic hydrocarbons, drugs	−0.77 to 4.81
[79]	Tissue:blood	Adipose tissue, liver, brain, kidney, muscle, lung, heart	Human	Alcohols, alkanes, ethers, fluorated ethers, alkenes, aromatic hydrocarbons, drugs	−4.62 to 6.80
[74]	Tissue:unbound plasma	Adipose tissue, bone, brain, intestine, heart, kidney, liver, lung, muscle, pancreas, skin, spleen, thymus	Rat	Drugs	0.88 to 4.96
[76]	Tissue:plasma	Adipose tissue, bone, brain, intestine, heart, liver, lung, kidney, muscle, skin, spleen, testes	Rat	Drugs	−4.62 to 6.3

non-volatile environmental chemicals that are hydrophilic or that bind extensively to proteins.

3. QSARs of metabolic parameters for PBPK models

Metabolism in PBPK models is often described as a first order, second order or saturable process [3] (Table 8). The frequently employed description of enzymatic metabolism requires the knowledge of the maximum velocity of reaction ($V_{\max}$) and the Michaelis constant (*Km*, i.e. the affinity of the substrate for the metabolizing enzyme). In most situations of human exposure to environmental contaminants, the first order description, based on the use of intrinsic clearance ($CL_{\text{int}} = V_{\max}/Km$) or hepatic clearance ($CL_h$), is sufficient. The hepatic clearance CL_h is equal to the hepatic extraction ratio (i.e. the fraction of quantity of chemical extracted by the liver) times the volume of blood perfusing the liver per unit time (Q_L) [31]. The hepatic extraction ratio, E, in turn can be calculated on the basis of the intrinsic clearance (CL_{int}) and Q_L as follows [31]:

$$E = \frac{CL_h}{Q_L} = \frac{CL_{\text{int}}}{Q_L + CL_{\text{int}}} \tag{14}$$

where $CL_{\text{int}} = \frac{V_{\max}}{Km + C_v}$ and C_v is the free concentration of chemical at the site of metabolism.

The *in silico* approaches for predicting metabolic rates generally focus on two aspects: (1) identification of substrate specificity and (2) prediction of $V_{\max}$, Km, CL_{int} or CL_h. Much of the activity so far has focused on CYP-mediated metabolism. The literature is abundant with approaches and results regarding the modelling of protein structures and pharmacophores [3,5,12]; however, very little progress has been made in terms of QSARs for predicting metabolism parameters (e.g. CL_h, E, CL_{int}, $V_{\max}$, or Km) required for PBPK modelling of environmental chemicals. Whereas the lessons learnt with (Q)SAR modelling of drug metabolism are useful for orienting work on the development of (Q)SARs for environmental contaminants, there are some obvious limitations. A fundamental one

Table 8. Descriptions of the rate of metabolism in PBPK models.

Metabolic constants	*Description*
$V_{\max}$ and Km	$\frac{V_{\max} \cdot Cvl}{Km + Cvl}$
CL_{int}	$CL_{\text{int}} \cdot Cvl$
CL_h	$CLh \cdot Ca$
E	$Ql \cdot E \cdot Ca$

$V_{\max}$: maximal velocity of enzymatic reaction (mg h^{-1} or mmol h^{-1}); Km: Michaelis–Menten affinity constant (mg L^{-1} or mmol L^{-1}); CL_{int}: intrinsic clearance (L h^{-1}); CL_h: hepatic clearance (L h^{-1}); E: hepatic extraction ratio; Q_l: blood flow rate to liver (L h^{-1}); Cvl: concentration of chemical in venous blood leaving liver (mg L^{-1} or mmol L^{-1}); Ca: arterial blood concentration (mg L^{-1} or mmol L^{-1}).

Downloaded by [Montana State University Bozeman] at 08:07 20 August 2014

Downloaded by [Montana State University Bozeman] at 08:07 20 August 2014

relates to the major isoforms of CYP involved in metabolism. Contrary to the major isozymes involved in the metabolism of pharmaceuticals (CYP2D6, CYP3A4, CYP2C19, CYP1A2), the metabolism of environmental chemicals is principally mediated by: CYP1A1 (e.g. polycyclic aromatic hydrocarbons), CYP1B1 and CYP1A2 (e.g. aromatic amines), CYP2E1 (trichloroethylene, chloroform) as well as CYP3A4 to a limited extent (e.g. larger molecules) [98]. This aspect might be critical with regard to both qualitative predictions and quantitative prediction of the metabolism of environmental chemicals in biota.

For identifying substrates that can bind to or be metabolized by a given isozyme, a SAR component is often used. Basically, the intent here is to use the information on the active site of the enzyme (protein) and/or molecular structure or features of known substrates to infer about whether or not a particular chemical would be a substrate for a given isozyme. In this regard, visual inspection of the crystal structure, protein homology models and other descriptions of the active site are useful in understanding the structural requirements of molecules that fit into the enzymes or binding sites [99]. Mackman et al. [100] reported that the active site of CYP2E1 (an isozyme involved in the metabolism a number of low molecular weight air and water pollutants) is open to a height of 10 Å directly above the iron atom, and that the active site cavity (topologically congruent in both rats and humans) is primarily located above the pyrrole rings A and D, with the region above the pyrrole ring D being the most accessible. Lewis [101,102] proposed decision trees to identify the human CYP isozymes that can metabolize a given substrate (mostly drugs) using selected molecular descriptors ($\log P$, HOMO-LUMO, molecular area, depth or volume), and these are likely to be a useful starting point for identifying isozyme specificity of the metabolism of environmental chemicals.

The results of the step above, i.e. identification of pathways(s) and/or enzyme(s) involved in the metabolism of a set of chemicals, would be useful in guiding the development of QSARs for enzymic metabolism, induction or inhibition, as learnt from past work with drugs [1,20,99–105]. QSARs have been developed to predict the hepatic clearance of benzodiazepines in humans on the basis of physicochemical, electrostatic and steric molecular descriptors such as the difference between the lowest unoccupied and highest occupied molecular orbital energies, the ionization potential, the number of potential hydrogen bond donor atoms in the molecule, the geometry-optimized minimum internal energy, and $\log P$ [101]. The *in vitro* intrinsic clearance and human hepatic clearance of drugs have been modelled using 10 or more molecular descriptors calculated by specialized software [106,107]. The QSAR developed by Li et al. [106] predicted the human hepatic clearance from 13 molecular descriptors (cosmic torsional energy; inertia moment 2 length; dipole moment Z component; Kier ChiV4 (cluster) index; number of H-bond acceptors; six-membered rings; group count for methyl; ADME violations; energy of the lowest unoccupied molecular orbital (VAMP LUMO); energy of the highest occupied molecular orbital (VAMP HOMO); VAMP total dipole; VAMP dipole Z component; VAMP octupole ZZZ). Nikolic and Agababa [107] used partial least squares regression (PLSR) to select most relevant molecular descriptors for QSAR modelling of human microsomal intrinsic clearance and half-life of drugs (model 1: $r^2 = 0.84$, Q^2 leave-seven-out $= 0.62$; model 2: $r^2 = 0.808$, Q^2 leave-seven-out $= 0.63$). The models were calibrated using experimental data from 29 drugs. Model 1 used 10 molecular descriptors (molecular polarizability; bond information content; mean topological charge index of order 6; radial distribution function-4.5/weighted by atomic masses of the ligands; 3D-MoRSe-signal

24/weighted by atomic Sanderson electronegativities; third component symmetry directional weighted holistic invariant molecular (WHIM) index/unweighted; third component symmetry directional WHIM index/weighted by atomic masses; third component symmetry directional WHIM index/weighted by atomic Sanderson electronegativities; number of tertiary aromatic amines and atom centre = CR2 fragments), whereas model 2 used the same input parameters with the exception of the number of tertiary aromatic amines.

Binding to microsomal binding is another determinant that needs to be evaluated and modelled, particularly when metabolism data from *in vitro* test systems are used for extrapolating to *in vivo* situations. In this regard, Austin et al. [108] have developed a model that predicts the extent of non-specific binding to microsomal proteins using a modified lipophilicity descriptor ($\log P/D$) that accounts for the enhanced microsomal binding of basic compounds. This equation was calibrated for 37 drugs (20 bases, $-6.35 \leq \log P \leq 6.34$; 12 neutrals, $0.36 \leq \log P \leq 3.75$; and five acids, $2.86 \leq \log P \leq 4.81$) with less than 90% of compound unbound to microsomal proteins. Austin et al. [109] similarly modelled the extent of binding to hepatocytes based on data for 17 drugs (six bases, $1.99 \leq \log P \leq 5.14$; seven neutrals, $1.34 \leq \log P \leq 3.75$; and four acids, $3.21 \leq \log P \leq 4.81$) using either $\log P/D$ ($r^2 = 0.65$) or $\log D$ ($r^2 = 0.55$).

Even though there has historically been a general interest in the relationship between chemical structure and metabolic pathways of closely-related chemicals, there are only a few attempts to develop QSARs of CL_h, CL_{int}, V_{max} and Km of environmental pollutants. For example, Yin et al. [110] reported excellent correlations between biotransformation rates and calculated activation energies (ΔH_{act}) of CYP-mediated hydrogen abstractions for six halogenated alkanes (1-fluoro-1,1,2,2-tetrachloroethane, 1,1-difluoro-1,2,2-trichloroethane, 1,1,1-trifluoro-2,2-dichloroethane, 1,1,1,2-tetrafluoro-2-chloroethane, 1,1,1,2,2-pentafluoroethane, and 2-bromo-2-chloro-1,1,1-trifluoroethane) in both rat and human enzyme preparations. Loizou et al. [111] reported correlations between the rate of metabolism, $\log P$, polarizability and the activation enthalpy for four 1,1,1-trihaloethanes (1,1,1-trichloroethane, 1,1-dichloro-1-fluoroethane, 1-chloro-1,1-difluoroethane, and 1,1,1-trifluoroethane). Gargas et al. [112] studied the metabolism of 14 chlorinated organic volatile compounds (methanes, ethylenes and ethanes) using the gas uptake inhalation technique. They observed a ranking of the metabolic activity of methanes as a function of their degree of chlorination (CHCl3 > CH2Cl2 > CCl4). Such a trend was also observed with the ethylenes and the ethanes. Mortensen et al. [113] determined the *in vitro* metabolism rates and affinities for 25 hydrocarbons (aromatics, cycloalkanes, *n*-alkanes, 2-methylalkanes and 1-alkenes) containing 6 to 10 carbons. This study reported that the aromatic compounds were metabolized faster than the aliphatic hydrocarbons in terms of CL_{int}. The CL_{int} of the hydrocarbons decreased with increasing number of carbons with no generalizable relationship between metabolic rate and the solubility of the alkanes in water [113]. The lack of more robust analyses of metabolism rates of environmental chemicals may be due to the fact that an exhaustive database on these parameters (i.e. V_{max} and Km together) obtained using the same *in vivo* or *in vitro* protocol is essentially unavailable, and that it is worse when focusing on V_{max} and Km of chemicals metabolized by a specific pathway and/or isozyme. A summary of selected quantitative analysis between chemical structure or properties and metabolism rates of environmental chemicals is provided below.

Downloaded by [Montana State University Bozeman] at 08:07 20 August 2014

- Galliani et al. [114] reported that V_{max} for the microsomal *N*-demethylation of para-substituted *N*,*N*-dimethylanilines could be modelled as follows:

$$\log V_{max} = 0.39\pi - 0.94\sigma - 1.56 \qquad n = 12, \quad r^2 = 0.89, \quad s = 0.23 \tag{15}$$

where V_{max} is the maximal velocity of the microsomal *N*-demethylation of para-substituted *N*,*N*-dimethylaniline; π is the Hansch hydrophobic constant and σ is the Hammett constant.

The above relationship indicates that the V_{max} increases with the substituent lipophilicity and electron-donating capacity of the substituent [99]. Further, this work also developed a QSAR for *Km* values essential for describing saturable metabolism associated with these V_{max} values.

- Csanady et al. [115], analysing the apparent metabolism (epoxidation) rate (mg g^{-1} per h) of a series of alkenes (ethene, 1-fluoroethene, 1,1-difluoroethene, 1-chloroethene, 1,1-dichloroethene, *cis*-1,2-dichloroethene, *trans*-1,1-dichloroethene, 1,1,1-trichloroethene, perchloroethene, propene, isoprene, 1,3-butadiene and styrene), reported that it can be explained by the following molecular parameters: ionization potential, dipole moment and π-electron density, obtained either using a quantum chemical method or from the literature.
- Parham and Portier [116] developed a QSAR model for predicting the rate of metabolism of PCBs. The resulting linear regression model contained seven independent variables describing the steric properties of PCBs (*ortho*, *para*, *meta* positions of the chlorine in different carbon pairs). Using step-wise regression analysis of first order metabolism (hydroxylation) rates of PCBs in rats, either obtained from PBPK models ($n = 9$) or rat liver microsomes ($n = 25$), these authors reported the following quantitative relationship ($r^2 = 0.9606$):

$$\begin{aligned}\text{Log rate} = {} & 0.4861(\pm 0.2034) - 0.1364(\pm 0.0267)\text{PL} \times \text{NSIDE} + 0.5694(\pm 0.1638)\text{UNS} \\ & - 0.2433 \times (\pm 0.0487)\text{NOM} \times \text{NOC} - 0.1544(\pm 0.0384)\text{NOM} \times \text{NMC} \\ & + 0.001227(\pm 0.000236)\text{MW} \times \text{NUNSTOT} + 0.8242(\pm 0.1297)\text{IND} \\ & - 1.1493(\pm 0.1438)\text{MOD}\end{aligned} \tag{16}$$

where PL is a descriptor of noncoplanarity; NSIDE is the number of *meta* (3, 5, 3′or 5′) chlorines plus the number of *para* (4 or 4′) chlorines; UNS is an indicator variable that is equal to 1 if there are any adjacent unsubstituted *meta* and *para* carbons; NOM is the number of adjacent unsubstituted *ortho-meta* carbons pairs; NOC is the number of ortho (2,6,2′ or 6′) chlorines; NMC is the number of meta (3, 5, 3′ or 5′) chlorines; MW is the molecular weight; NUNSTOT is equal to the sum of NUNMP and NUNOM; NUNMP is the number of adjacent non-chlorine-substituted *meta-para* carbon pairs; NUNOM is the number of adjacent non-chlorine-substituted *ortho-meta* carbon pairs; IND is equal to 1 if the data point is from Aroclor-induced experiments and otherwise equal to 0; and MOD is equal to 1 if the data point is from model fit, otherwise equal to 0.

Downloaded by [Montana State University Bozeman] at 08:07 20 August 2014

- Gargas et al. [60] attempted to develop a QSAR for the V_{max} of 16 halogenated methanes, ethanes and ethylenes using higher order molecular connectivity indices as follows:

$$\log V_{max} = 1.676(\pm 0.049)^4 \chi_c^v + 0.424(\pm 0.110)^3 \chi_c^v - 0.134(\pm 0.045)^4 \chi_{pc}^v + 1.622(\pm 0.049). \quad (17)$$

The use of first-order connectivity indexes gave relatively better results for the prediction of $\log V_{max}$ ($r^2 = 0.905$, $s = 0.1355$, $n = 16$, $p < 0.0001$) but the predictive power and robustness of the QSAR were questionable. Furthermore, since *Km* values were not successfully modelled in this study, the V_{max} alone could not be used for PBPK modelling.

- QSARs were also developed for the V_{max} (three models) and V_{max}/Km of a series of seven alkylbenzene compounds (toluene, *o*-, *m*, *p*-xylene, ethylbenzene, 1,2,4-trimethylbenzene, styrene), all substrates of CYP2E1 [117]. The input parameters used in the QSARs were the $\log P$ for $\log V_{max}/Km$, the ΔE (i.e. the difference between the energy of the highest unoccupied molecular orbital, ELUMO, and the energy of the lowest unoccupied molecular orbital, EHOMO) for the $\log V_{max}$ (model versions 1 and 3) or the ionization potential (*IP*) of the compound for $\log V_{max}$ (model 2):

$$\text{model 1: } \log V_{max} = 18.799 - 1.632(\pm 0.324)\Delta E \quad r^2 = 0.929, \quad s = 0.1197, \quad F = 19.08, \quad n = 6 \quad (18)$$

$$\text{model 2: } \log V_{max} = 18.955 - 1.741(\pm 0.345)IP \quad r^2 = 0.930, \quad s = 0.1195, \quad F = 19.14, \quad n = 6 \quad (19)$$

$$\text{model 3: } \log V_{max} = 44.301(\pm 7.803)\Delta E - 2.369(\pm 0.413)\Delta E^2 - 203.75 \quad r^2 = 0.954, \quad s = 0.0986, \quad F = 40.41, \quad n = 7 \quad (20)$$

- Knaak et al. [118], based on an initial analysis of the V_{max} and *Km* for the metabolism of dialkyl *p*-nitrophenyl phosphorothioates and phenyl substituted phosphorothioates to their oxons, reported the following relationships:

$$V_{max} = -0.05142(\text{MV}) + 18.63(\text{xp10}) + 0.279(\text{SdsO}) + 15.9665 \quad r^2 = 0.981, \quad n = 11, \quad F = 118.4, \quad \text{cross} - \text{validation RSS} = 13.44 \quad (21)$$

where MV is the molecular volume; xp10 is the simple connectivity index (10th-order path chi index); and SdO is the atom type E-state, sum of all (=0) in the molecule;

$$Km = -56.63(\text{ABSQ}) + 24.19(\text{SsCH}_3) + 2.222(\text{SsF}) + 40.3213 \quad r^2 = 0.9522, \quad n = 11, \quad F = 46.48 \quad (22)$$

where ABSQ is the 3D descriptor, sum of the absolute values of charges on each atom of molecule, in electrons; SsCH_3 is the atom type E-state, sum of all (CH_3) E-state values in

Downloaded by [Montana State University Bozeman] at 08:07 20 August 2014

the molecule; and SsF is the atom type E-state, sum of all (F) E-state values in the molecule.

In this study, however, cross-validation of the *Km* model was not possible even though the overall database included relevant pesticides such as parathion, chlorpyrifos, methyl parathion and isofenphos.

- Waller et al. [119] observed that there has been little success in the use of the energy of the LUMO or the energy of the HOMO, to predict the rates of oxidative or reductive metabolism, even though the propensity of chemicals metabolized by these process is indicated by the electron affinity or the ionization potential. Applying a CoMFA analysis to a set of 12 VOCs metabolized principally by CYP2E1 (chloromethane, dichloromethane, chloroform, carbon tetrachloride, chloroethylene, 1,1-dichloroethylene, *cis*-1,2-dichloroethylene, *trans*-1,2-dichloroethylene, trichloroethylene, chloroethane, 1,2-dichloroethane, 1,2-dichloroethane), these authors reported that the combination of steric, electrostatic, LUMO and HINT hydropathicity fields was essential to adequately model the CL_{int} of this small set of environmental chemicals ($r^2 = 0.953$, $q^2 = 0.527$) [119]. Developing QSARs for CL_h in this regard would be particularly relevant, given that for highly metabolized chemicals, it is the blood flow rate and not the intrinsic clearance that would limit or determine the extent of hepatic metabolism [120–122].
- Béliveau et al. [62] developed a simpler, group contribution method to compute the *in vivo* CL_h of several relatively lipophilic VOCs (alkanes, haloalkanes, haloethylenes, and aromatic hydrocarbons) in rats. Similarly, Kamgang et al. [63] used the group contribution method to develop QSARs based on the enzyme-content normalized values of CL_{int} of alkanes, alkenes and aromatic hydrocarbons based on *in vitro* data of Mortensen et al. [113]. Table 9 presents the published values of group contributions to the hepatic and intrinsic clearance

Table 9. Fragment-specific contributions to the hepatic and intrinsic clearance for VOCs.[a]

	Contribution to	
Fragment	CL_h	CL_{int}
CH_3	0.388	−0.005
CH_2	−0.186	0.039
CH	−0.464	0.042
C	−1.440	−1.735
C=C	−1.710	0
H	0.813	0.039
Br	0.523	–
Cl	0.537	–
AC	0.128	0.825
H on AC	0.061	0.353

[a]The fragment-specific contributions times the frequency of their occurrence gives the particular metabolic constant. Based on Béliveau et al. [62] and Kamgang et al. [63].

Downloaded by [Montana State University Bozeman] at 08:07 20 August 2014

for VOCs. The intrinsic clearance normalized for P450 2E1 facilitates the extrapolation of the hepatic clearance between species by substituting the species-specific data (i.e. cytochrome P-450 content, volume of liver, hepatic blood flow) in the following equation [81]:

$$CL_h = Q_L \cdot \frac{CL_{\text{int, P450}} \cdot [\text{P450}] \cdot V_L}{Q_L + CL_{\text{int, P450}} \cdot [\text{P450}] \cdot V_L} \tag{23}$$

where [P450] corresponds to the concentration of cytochrome P-450 in the liver; V_L is the liver volume; Q_L is the blood flow to liver; and $CL_{\text{int, P450}}$ is the intrinsic clearance normalized for P-450 content.

Limited efforts have focused on the integration of the QSARs for partition coefficients and metabolism constants described in the preceding sections along with human or animal physiology information to predict the pharmacokinetics of environmental chemicals using the PBPK model framework, as discussed below.

Downloaded by [Montana State University Bozeman] at 08:07 20 August 2014

4. QSAR-PBPK modelling

The bottleneck for developing PBPK models for emerging or known environmental contaminants is the chemical-specific input parameters. At the present time, based primarily on research and development in the pharmaceutical arena, a number of QSAR tools have become available to facilitate the prediction of drug absorption, distribution and clearance but not the actual time-course of the drug or metabolite concentration in the target site or blood for various dosing regimens and species. In this context, Blakey et al. [123] developed PBPK models for a homologous series of barbiturates in the rat, focusing on the change in pharmacokinetics and increase in lipophilicity of the congeners due to the addition of methylene group. Regarding environmental chemicals, however, there does not exist a suite of adequate *in silico* approaches to generate *a priori* the values of ADME parameters to facilitate high-throughput PBPK modelling.

Overall, the use of the PBPK modelling framework for simulating pharmacokinetics of a given chemical requires the numerical values of physiological, physicochemical and biochemical parameters [62,63,81,86,120,124]. Whereas the physiological parameters can be obtained from the literature, the other parameters can be estimated using QSARs as detailed above. The PCs required for PBPK modelling can be estimated from molecular structure information but reliable estimates of metabolic constants for environmental chemicals are often unavailable. In such cases, a pragmatic approach involves setting the numerical value of hepatic extraction ratio, E, to 0 or 1 in PBPK models, along with QSAR-driven estimates of PCs. This approach, based on the use of the theoretical physiological limits of metabolism (i.e. zero and liver blood flow), has been demonstrated to be useful for inhaled environmental toxicants [120]. The resulting simulations reflect 'bounds' of the blood concentrations of chemicals reflective of the fact that the liver cannot remove more than what is delivered by the blood flowing to the tissue (i.e. the value of hepatic extraction ratio, E, cannot exceed 1) and that the E value cannot be lower than 0. The strategy here involves the specification of the values of physiological parameters and QSARs for PCs in the PBPK model and setting of E value to 0 or 1 in the metabolism equation. The envelope of blood concentration profiles predicted by such an approach will, in principle, encompass all experimental data [120]. For example, using the human QSAR-PBPK model [81,120], the envelope of blood concentration of trichloroethylene (1

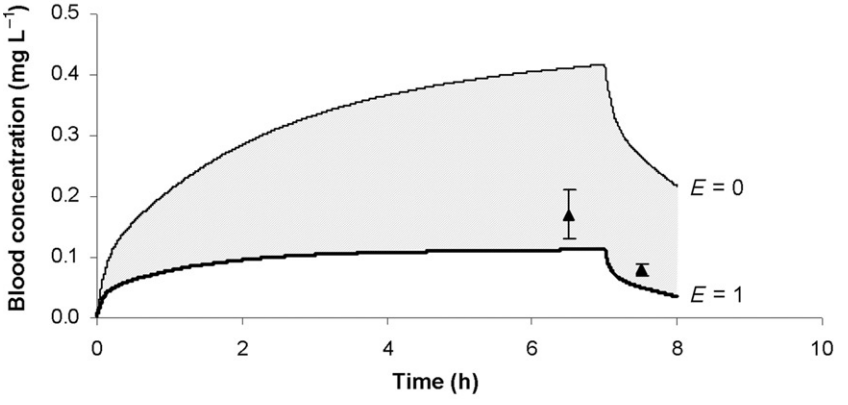

Figure 4. Comparison between the experimental data (symbols) and the envelope of trichloroethylene venous blood concentration simulated by human QSAR-PBPK model (exposure condition: 12.1 ppm, 7 h) [120] using values of 0 and 1 for the hepatic extraction ratio (E).

Downloaded by [Montana State University Bozeman] at 08:07 20 August 2014

C=C, 1 H, 3 Cl) following 7 h exposure to 12.1 ppm was simulated by setting the value of E equal to 0 and then to 1 (Figure 4). The use of the range of E is also justified by the fact that metabolic rates might be variable among individuals but will necessarily be within the range of 0 to 1. Further, this approach implicitly considers the impact of pharmacokinetic interactions during mixed exposures. When the hepatic metabolism of a chemical is reduced (or enhanced) due to enzyme inhibition (or induction), the E value will change but never exceed 1 or be lower than 0. Introducing the QSARs for computing route-specific absorption rates can extend the current capability of this QSAR-PBPK modelling approach, which is limited to the inhalation route. In this regard a number of algorithms and commercial software are available to provide estimates of skin permeability coefficient as well as oral absorption rates (e.g. [125–131]).

A logical and more refined alternative to the prediction of the envelope of the range of blood concentrations would involve the use of QSARs to specify an appropriate or approximate value of the rate of metabolism for a given chemical in the PBPK model. When QSARs for both partition coefficients and metabolism rates are available, the prediction of the pharmacokinetic profiles and internal dose of chemicals has been accomplished with the PBPK modelling framework using one of two approaches (Figure 5). The first approach involves the development of 'species-specific' QSARs for blood:air, tissue:blood and hepatic clearance parameters, and their integration within the PBPK model such that the numerical values of these input parameters are generated automatically during simulations only from molecular structure provided as input [62,86,120]. According to this approach, then, instead of providing experimentally-determined PCs or metabolic constants as input to the PBPK model, all one has to do is to change the number and/or nature of fragments in the molecule to estimate chemical-specific input parameters required for modelling its pharmacokinetics in a specific species (i.e. rat or human). This QSAR-PBPK approach has been investigated by Béliveau et al. [62] using inhaled VOCs in the rat. These authors used Free–Wilson type QSPR models to predict the chemical-specific input parameters (liver:air, richly perfused tissues:air, poorly perfused tissues:air, and fat:air PCs and hepatic clearance), and incorporated them with the PBPK model to predict the inhalation pharmacokinetics of eight VOCs (four from the

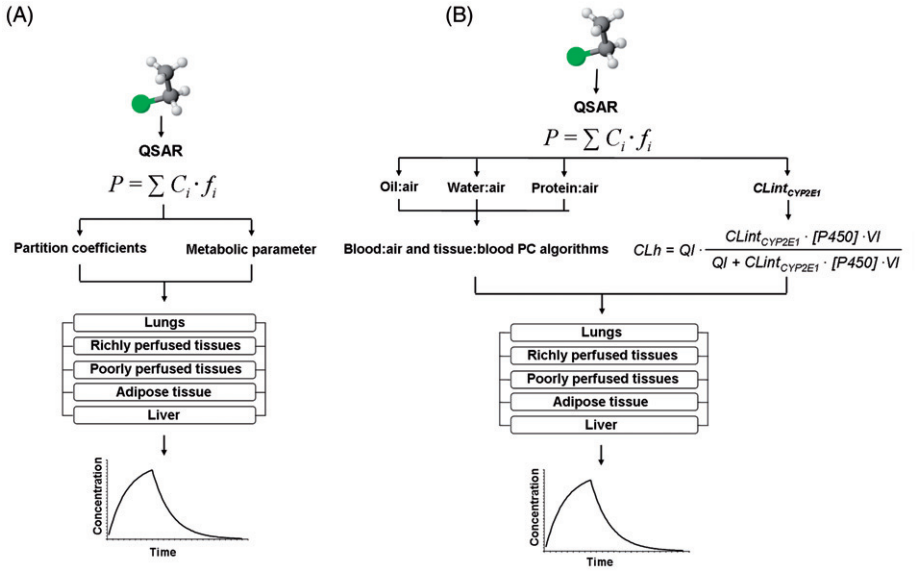

Figure 5. Illustration of the two approaches (A, B) for the development of PBPK models based on QSARs for chemical-specific input parameters.

Downloaded by [Montana State University Bozeman] at 08:07 20 August 2014

calibration set: toluene, dichloromethane, trichloroethylene, and 1,1,1-trichloroethane; four outside the calibration set: 1,2,4-trimethylbenzene, ethylbenzene, 1,3-dichloropropene, and 2,2- dichloro-1,1,1-trifluoroethane). For example, to simulate the kinetics of toluene in rat with this QSAR-PBPK model, the frequency of occurrence of molecular fragments (i.e. $1 \times$ CH3, $1 \times$ AC, and $5 \times$ H on AC) was entered as input to the model along with their respective contributions to PCs (Table 2). The Free–Wilson model then yields the following blood:air and tissue:blood partition coefficients for toluene in the rat [62]:

- Blood:air PC $= 10^{[1\times0.072+1\times2.850+5\times(-0.292)]} = 29$;
- Liver:blood PC $= 10^{[1\times0.016+1\times3.760+5\times(-0.408)]}/29 = 1.88$; and
- Muscle:blood PC $= 10^{[1\times(-0.020)+1\times3.650+5\times(-0.446)]}/29 = 0.87$.

Similarly, the metabolic clearance of toluene can be computed using the molecular fragments contained in toluene (i.e. $1 \times$ CH3, $1 \times$ AC, and $5 \times$ H on AC) along with the group contributions listed in Table 9, as follows [62]:

- $CL_h = 1 \times 0.388 + 1 \times 0.128 + 5 \times 0.061 = 0.82\ \mathrm{L\,h^{-1}}$.

Using the above chemical-specific parameters along with rat physiological parameters (volumes of liver, fat, richly perfused tissues, and poorly perfused tissues respectively equal 0.012, 0.022, 0.012, and 0.174 L; blood flow to liver, fat, richly perfused tissues, and poorly perfused tissues equal 1.31, 0.47, 2.68, and 0.79 $\mathrm{L\,h^{-1}}$, respectively; cardiac output and alveolar ventilation $= 5.25\ \mathrm{L\,h^{-1}}$), the QSAR-PBPK model simulated the toluene kinetics in blood in rats exposed to 50 ppm for 4 h (Figure 6) [62]. Since the metabolic input

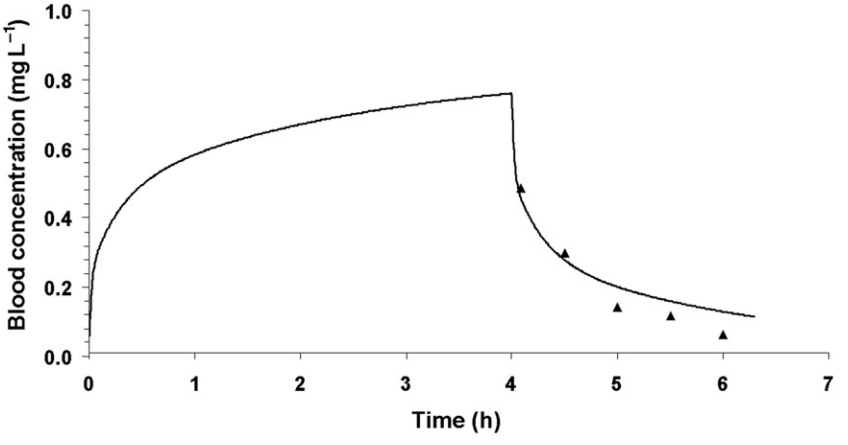

Figure 6. Comparison between the experimental data (symbols) and the QSAR-PBPK model predictions (solid line) of toluene venous blood concentration for 50 ppm, 4 h inhalation exposure in rat. Based on Béliveau et al. [62].

Downloaded by [Montana State University Bozeman] at 08:07 20 August 2014

parameters did not correspond to V_{max} and *Km*, this model is of use only under first order conditions, i.e. it is not useful for conducting high dose to low dose extrapolation, to simulate the impact of metabolic saturation on internal dose of toluene.

Another methodological approach in QSAR-PBPK modelling relates to developing chemical-specific parameters that are independent of the species and then integrating them with species-specific parameters (e.g. tissue composition data) such that distribution volume and pharmacokinetic profiles can be predicted (Figure 5B). This approach is exemplified by the work of Béliveau et al. [81]. These authors conducted interspecies extrapolations of the inhalation toxicokinetics of VOCs using the same PBPK model for which the input parameters were predicted using QSARs along with species-specific biological data. Thus, the results of the QSARs for oil:air, water:air and protein:air PCs were used as input for the computation of the blood:air and tissue:blood PCs whereas the QSAR for intrinsic clearance was incorporated along with CYP content and volume of liver in an algorithm for computing hepatic clearance. For toluene, as example, the use of occurrence of fragments in the molecule (i.e. 1 CH3, 1 AC, and 5 H on AC) along with the group contributions listed in Table 5, the oil:air, water:air and protein:air PCs are computed as follows [81]:

- Oil:air PC $= 10^{[1\times0.354+1\times3.729+5\times(-0.190)]} = 1358$;
- Water:air PC $= 10^{[1\times(-0.038)+1\times0.650+5\times(-0.062)]} = 2$; and
- Protein:air PC $= 10^{[1\times0.306+1\times1.970+5\times(-0.028)]} = 136.6$.

Then, incorporating these partition coefficients along with rat tissue and blood composition (Table 4) in the tissue composition-based algorithms (Equations (12) and (13)), the following values of PCs are obtained within the QSAR-PBPK model:

- Blood:air PC $= 1358 \times 0.002 + 2 \times 0.8423 + 137 \times 0.156 = 26$;
- Liver:blood PC $= (1358 \times 0.0425 + 2 \times 0.7176)/26 = 2.3$; and
- Muscle:blood $= (1358 \times 0.0117 + 2 \times 0.7471)/26 = 0.68$

Table 10. Fragment-specific contributions to intrinsic clearance normalized to P450 CYP2E1 content in liver.[a]

Fragment in molecule	*Contribution to* $\log CL_{int}$ *(CYP2E1)*
CH_3	1.552
CH_2	0.514
CH	0.078
C	−0.871
C=C	0.591
H	0.383
Br	1.000
Cl	0.522
F	0.000
AC	−7.646
H on AC	1.535

[a]Based on Béliveau et al. [81].

Downloaded by [Montana State University Bozeman] at 08:07 20 August 2014

The intrinsic clearance, normalized to CYP2E1 content in liver, can be calculated using the occurrence of fragments in toluene molecule and the corresponding fragment contributions (Table 10) as follows [81]:

- $CLint_{CYP2E1} = 10^{[1\times1.552+1\times(-7.646)+5\times1.535]} = 38\,\mathrm{L\,h^{-1}}$ per μmol CYP2E1.

The QSAR-based intrinsic clearance ($2.19\,\mathrm{L\,h^{-1}}$) was then obtained by multiplying the above $CLint_{CYP2E1}$ value with the hepatic concentration of CYP2E1 ($4.8\,\mu\mathrm{mol\,L^{-1}}$) and the volume of liver (0.012 L) in rats.

The blood:air and tissue:blood PCs computed using QSARs and species-specific biological data feed into the various equations to provide pharmacokinetic simulations (Figure 5B). The QSAR-PBPK model was initially used to predict the blood kinetic profile of inhaled toluene in rats (50 ppm, 4 h) (Figure 7A); thereafter by changing only the species-specific physiological data (human tissue and blood compositions reported in Table 4; hepatic concentration of cytochrome P450 2E1 = $2.482\,\mu\mathrm{mol\,L^{-1}}$; volumes of liver, fat, richly perfused tissues, and poorly perfused tissues = 1.82, 13.3, 3.5, and 43.4 L, respectively; blood flows to liver, fat, richly perfused tissues, and poorly perfused tissues = 108, 20.9, 184, and $104\,\mathrm{L\,h^{-1}}$, respectively; cardiac output and alveolar ventilation = $417\,\mathrm{L\,h^{-1}}$), simulations of kinetics in humans (17 ppm, 7 h) were obtained with the same QSPR-PBPK model (Figure 7B) [81].

The QSAR-PBPK models developed for rats and humans can also be adopted for other species. In this regard, for example, the chemical-specific parameters of the PBPK model for chloroethanes developed for fish [42] can be replaced with the results of QSAR modelling. The log *P* as well as tissue composition data can be used together to compute PCs of 1,1,2,2-tetrachloroethane ($\log P = 2.39$, blood:water = 7.8, fat:blood = 37.3, liver:blood = 1.17, muscle:blood = 1.37) in rainbow trout [42,83]. Incorporating these results with data on fish physiology within a PBPK model, it becomes possible to generate a first-cut simulation of the kinetic profile of 1,1,2,2-tetrachloroethane in fish (Figure 8).

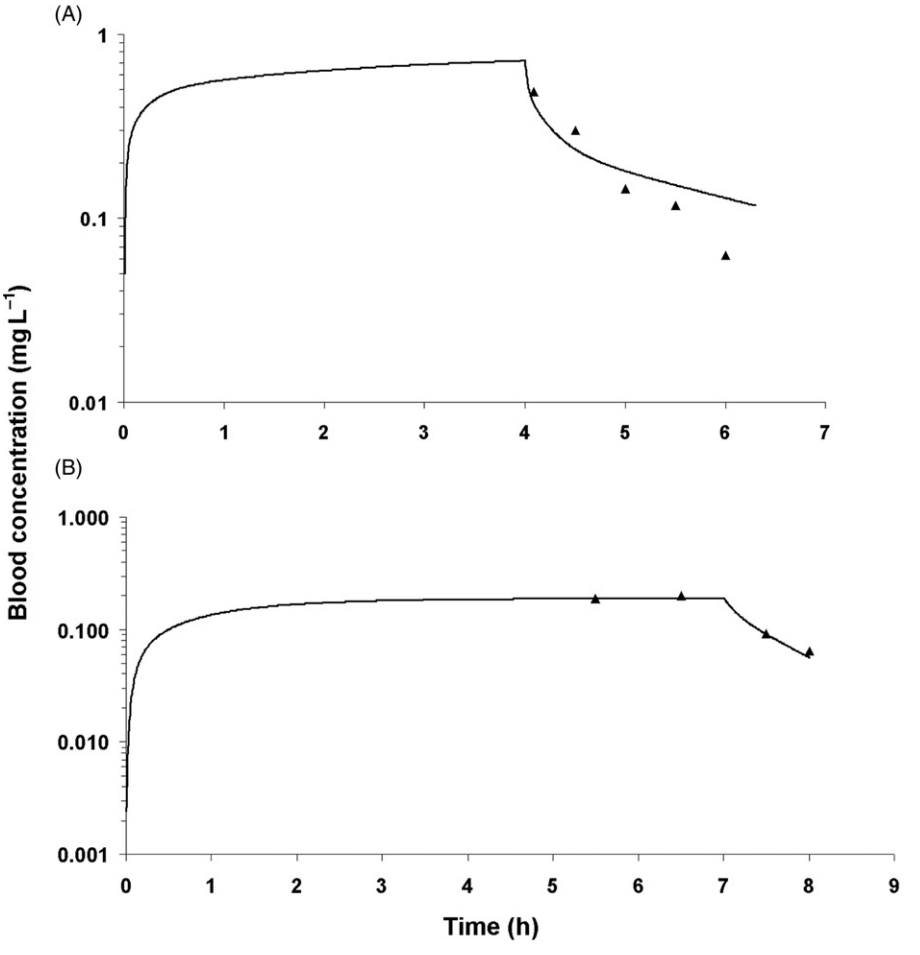

Figure 7. Comparison between the experimental data (symbols) and the QSAR-PBPK model predictions (solid line) of toluene venous blood concentration for inhalation exposures. (A) 50 ppm, 4 h in the rat; (B) 17 ppm, 7 h in humans. Based on Béliveau et al. [81].

5. Conclusions

The current paradigm shift in toxicology and risk assessment would benefit from the availability of tools and approaches for generating pharmacokinetic and internal dose information. For data-poor chemicals and situations, it is relevant to explore the use of QSAR-based approaches to provide simulations of pharmacokinetics. The development of SARs and QSPRs for the input parameters of PBPK models will not only facilitate the prediction of the internal dose of a given chemical but also the development of internal dose-based toxicodynamic QSARs of relevance to risk assessment (e.g. [132]). Importantly, all of this can be done solely with knowledge of molecular structure or properties and understanding of the underlying mechanisms. Until now, physicochemical and biochemical parameters required for PBPK modelling have mostly been obtained by conducting *in vivo* or *in vitro* studies. With the more recent advances and algorithms

Downloaded by [Montana State University Bozeman] at 08:07 20 August 2014

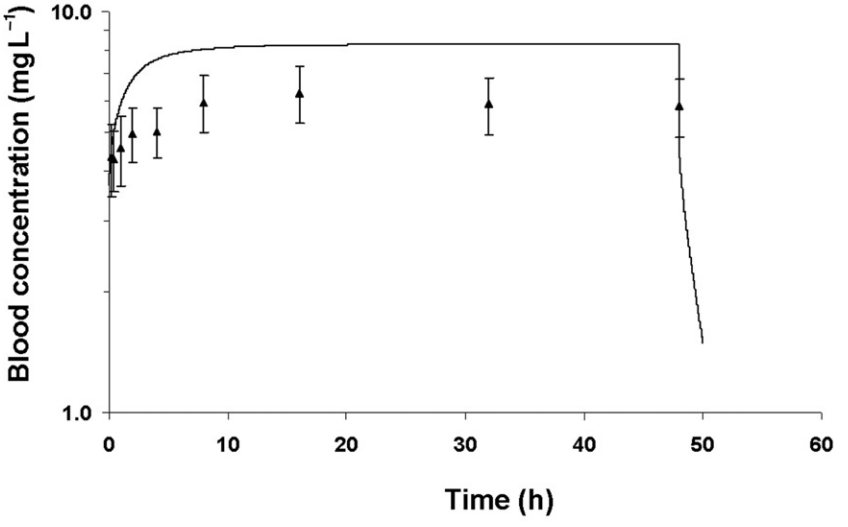

Figure 8. Comparison between the experimental data (symbols) and the QSAR-PBPK predictions (solid line) of arterial blood concentration in rainbow trout exposed to 1.06 mg 1,1,2,2-tetrachloroethane/L water during 48 h. Data from Nichols et al. [42].

Downloaded by [Montana State University Bozeman] at 08:07 20 August 2014

reviewed in this article, it is clear that chemical-specific parameters such as physicochemical and biochemical constants can be estimated from information on molecular structure. *In silico* approaches for estimating PBPK model parameters have mainly centred on LFE-type QSARs and mechanistic algorithms. The application of LFE QSARs, however, is limited to the biological species in which the data are collected. It is important that mechanistic relevance of the structural descriptors used in these types of equations to the *in vivo* pharmacokinetics of chemicals be developed. The emerging mechanistically-based algorithms offer the potential of being applicable to multiple chemical families as well as multiple levels of organization (e.g. cells, organs, species, populations). However, these approaches should further evolve to account for the uncertainty and variability in input parameters, by applying a distributional rather than a deterministic approach to QSAR-PBPK modelling. Even though the development of QSAR-PBPK approaches has largely been limited to inhaled VOCs, they are conceptually applicable to non-volatile organics as well, but it becomes more challenging to predict the other PBPK model parameters required for modelling the kinetics of the latter (i.e. tissue diffusion coefficients, association constants for binding, oral absorption rates, and dermal permeability coefficients). As our level of understanding of the mechanistic determinants of each of these parameters improves, we can be optimistic of being able to develop mechanistic QSARs to provide *a priori* predictions of these parameters and ultimately the *in vivo* pharmacokinetics of new chemicals, ahead of laboratory evaluations.

Acknowledgements

The authors wish to acknowledge the grants from ANSES (EST-2007-85) and NSERC (operating grant) to pursue research on the development of QSAR-PBPK models.

Downloaded by [Montana State University Bozeman] at 08:07 20 August 2014

References

[1] C. Hansch, A. Leo, and D.H. Hoekman, *Exploring QSAR*, American Chemical Society, Washington, DC, 1995.

[2] J.M. Mayer and H. van de Waterbeemd, *Development of quantitative structure-pharmacokinetic relationships*, Environ. Health Perspect. 61 (1985), pp. 295–306.

[3] J.K. Seydel and K.J. Schaper, *Quantitative structure–pharmacokinetic relationships and drug design*, Pharmacol. Ther. 15 (1981), pp. 131–182.

[4] A.M. Davis and R.J. Riley, *Predictive ADMET studies, the challenges and the opportunities*, Curr. Opin. Chem. Biol. 8 (2004), pp. 378–386.

[5] S. Ekins, G. Bravi, B.J. Ring, T.A. Gillespie, J.S. Gillespie, M. Vandenbranden, S.A. Wrighton, and J.H. Wikel, *Three-dimensional quantitative structure activity relationship analyses of substrates for CYP2B6*, J. Pharmacol. Exp. Ther. 288 (1999), pp. 21–29.

[6] S. Ekins and R.S. Obach, *Three-dimensional quantitative structure activity relationship computational approaches for prediction of human in vitro intrinsic clearance*, J. Pharmacol. Exp. Ther. 295 (2000), pp. 463–473.

[7] S. Ekins and J. Rose, *In silico ADME/Tox: The state of the art*, J. Mol. Graph. Model. 20 (2002), pp. 305–309.

[8] S. Ekins, C.L. Waller, P.W. Swaan, G. Cruciani, S.A. Wrighton, and J.H. Wikel, *Progress in predicting human ADME parameters in silico*, J. Pharmacol. Toxicol. Meth. 44 (2000), pp. 251–272.

[9] C. Hansch, S.B. Mekapati, A. Kurup, and R.P. Verma, *QSAR of cytochrome P450*, Drug Metab. Rev. 36 (2004), pp. 105–156.

[10] T. Hou and J. Wang, *Structure-ADME relationship: Still a long way to go?*, Expert Opinion Drug Metabol. Toxicol. 4 (2008), pp. 759–770.

[11] J. Ishizaki, K. Yokogawa, E. Nakashima, and F. Ichimura, *Relationships between the hepatic intrinsic clearance or blood cell-plasma partition coefficient in the rabbit and the lipophilicity of basic drugs*, J. Pharm. Pharmacol. 49 (1997), pp. 768–772.

[12] J. Langowski and A. Long, *Computer systems for the prediction of xenobiotic metabolism*, Adv. Drug Deliv. Rev. 54 (2002), pp. 407–415.

[13] D.F. Lewis and M. Dickins, *Baseline lipophilicity relationships in human cytochromes P450 associated with drug metabolism*, Drug Metab. Rev. 35 (2003), pp. 1–18.

[14] H. Li, J. Sun, X. Fan, X. Sui, L. Zhang, Y. Wang, and Z. He, *Considerations and recent advances in QSAR models for cytochrome P450-mediated drug metabolism prediction*, J. Comput. Aided Mol. Des. 22 (2008), pp. 843–855.

[15] N. Manga, J.C. Duffy, P.H. Rowe, and M.T.D. Cronin, *A hierarchical QSAR model for urinary excretion of drugs in humans as a predictive tool for biotransformation*, QSAR Comb. Sci. 22 (2003), pp. 263–273.

[16] D.E. Mager, *Quantitative structure-pharmacokinetic/pharmacodynamic relationships*, Avd. Drug Delivery Rev. 58 (2006), pp. 1326–1356.

[17] U. Norinder, *In silico modelling of ADMET – a minireview of work from 2000 to 2004*, SAR QSAR Environ. Res. 16 (2004), pp. 1–11.

[18] T. Wang and J. Hou, *Recent advances on in silico ADME modeling*, Ann. Reports Comput. Chem. 5 (2009), pp. 101–127.

[19] Y.-H. Wang, Y. Li, Y.-H. Li, S.-L. Yang, and L. Yang, *Modeling Km values using electrotopological state: Substrates for cytochrome P450 3A4-mediated metabolism*, Bioorg. Med. Chem. Lett. 15 (2005), pp. 4076–4084.

[20] C.W. Yap, Z.R. Li, and Y.Z. Chen, *Quantitative structure-pharmacokinetic relationships for drug clearance by using statistical learning methods*, J. Mol. Graph. Model. 24 (2006), pp. 383–395.

[21] K. Krishnan and M.E. Andersen, *Physiologically based pharmacokinetic modeling in toxicology*, in *Principles and Methods of Toxicology*, A.W. Hayes, ed., Taylor & Francis, Boca Raton, FL, 2007, pp. 231–292.

[22] M.E. Andersen, H.J. Clewell, M.L. Gargas, F.A. Smith, and R.H. Reitz, *Physiologically based pharmacokinetics and the risk assessment process for methylene chloride*, Toxicol. Appl. Pharmacol. 87 (1987), pp. 185–205.
[23] M. Reddy, R.S. Yang, M.E. Andersen, and H.J. Clewell III (eds.), *Physiologically Based Pharmacokinetic Modeling: Science and Applications*, Wiley Interscience, Hoboken, N.J., 2006, pp. 1–420.
[24] G. Loizou, M. Spendiff, H.A. Barton, J. Bessems, F.Y. Bois, M.B. d'Yvoire, H. Buist, H.J. Clewell, B. Meek, U. Gundert-Remy, G. Goerlitz, and W. Schmitt, *Development of good modelling practice for physiologically based pharmacokinetic models for use in risk assessment: The first steps*, Regul. Toxicol. Pharmacol. 50 (2008), pp. 400–411.
[25] A.D. Arms and C.C. Travis, *Reference physiological parameters in pharmacokinetic modeling*, in *EPA/600/6-88/004*, U.S. Environmental Protection Agency, Office of Health and Environmental Assessment, Washington, DC, 1988.
[26] R.P. Brown, M.D. Delp, S.L. Lindstedt, L.R. Rhomberg, and R.P. Beliles, *Physiological parameter values for physiologically based pharmacokinetic models*, Toxicol. Ind. Health 13 (1997), pp. 407–484.
[27] T. Lavé, P. Coassolo, and B. Reigner, *Prediction of hepatic metabolic clearance based on interspecies allometric scaling techniques and in vitro–in vivo correlations*, Clin. Pharmacokinet. 36 (1999), pp. 211–231.
[28] J.W. Nichols, I.R. Schult, and P.N. Fitzsimmons, *In vitro–in vivo extrapolation of quantitative hepatic biotransformation data for fish. I. A review of methods, and strategies for incorporating intrinsic clearance estimates into chemical kinetic models*, Aquat. Toxicol. 78 (2006), pp. 74–90.
[29] M. Béliveau and K. Krishnan, *In silico approaches for developing physiologically based pharmacokinetic (PBPK) models*, in *Alternative Toxicological Methods*, H. Salem and S.A. Katz, eds., CRC Press, Boca Raton, FL, 2003, pp. 479–532.
[30] P. Poulin, M. Béliveau, and K. Krishnan, *Mechanistic animal replacement appoaches for predicting pharmacokinetics of organic chemicals*, in *Toxicity Assessment Alternatives: Methods, Issues, Opportunities*, H. Salem and S.A. Katz, eds., Humana Press, Totowa, NJ, 1999, pp. 115–139.
[31] M. Gibaldi and B. Perrier, *Pharmacokinetics*, Dekker, New York, 1975.
[32] M.H. Abraham, M.J. Kamlet, R.W. Taft, R.M. Doherty, and P.K. Weathersby, *Solubility properties in polymers and biological media. 2. The correlation and prediction of the solubilities of nonelectrolytes in biological tissues and fluids*, J. Med. Chem. 28 (1985), pp. 865–870.
[33] A. Falk, E. Gullstrand, A. Löf, and E. Wigaeus-Hjelm, *Liquid/air partition coefficients of four terpenes*, Br. J. Ind. Med. 47 (1990), pp. 62–64.
[34] R.M. Featherstone, C.A. Muehlbaecher, F.L. Debon, and J.A. Forsaith, *Interactions of inert anesthetic gases with proteins*, Anesthesiology 22 (1961), pp. 977–981.
[35] V. Fiserova-Bergerova and M.L. Diaz, *Determination and prediction of tissue–gas partition coefficients*, Int. Arch. Occup. Environ. Health 58 (1986), pp. 75–87.
[36] V. Fiserova-Bergerova, M. Tichy, and F.J. Di Carlo, *Effects of biosolubility on pulmonary uptake and disposition of gases and vapors of lipophilic chemicals*, Drug Metab. Rev. 15 (1984), pp. 1033–1070.
[37] M.L. Gargas, R.J. Burgess, D.E. Voisard, G.H. Cason, and M.E. Andersen, *Partition coefficients of low-molecular-weight volatile chemicals in various liquids and tissues*, Toxicol. Appl. Pharmacol. 98 (1989), pp. 87–99.
[38] J. Järnberg and G. Johanson, *Liquid/air partition coefficients of the trimethylbenzenes*, Toxicol. Ind. Health 11 (1995), pp. 81–88.
[39] T. Kaneko, P.Y. Wang, and A. Sato, *Partition coefficients of some acetate esters and alcohols in water, blood, olive oil, and rat tissues*, Occup. Environ. Med. 51 (1994), pp. 68–72.
[40] C.P.J.M.D. Larson, E.I.I.M.D. Eger, and J.W.M.D. Severinghous, *Ostwald solubility coefficients for anesthetic gases in various fluids and tissues*, Anesthesiology 23 (1962), pp. 686–689.
[41] H.J. Lowe and K. Hagler, *Determination of volatile organic anaesthetic in blood, gases, tissues and lipids: Partition coefficients*, in *Gas Chromatography in Biology and Medicine. A Ciba-Geigy Foundation Symposium*, R. Porter, ed., Churchill, New York, 1969, pp. 86–103.

Downloaded by [Montana State University Bozeman] at 08:07 20 August 2014

[42] J.W. Nichols, J.M. McKim, G.J. Lien, A.D. Hoffman, and S.L. Bertelsen, *Physiologically based toxicokinetic modeling of three waterborne chloroethanes in rainbow trout (Oncorhynchus mykiss)*, Toxicol. Appl. Pharmacol. 110 (1991), pp. 374–389.
[43] S. Paterson and D. Mackay, *Correlation of tissue, blood, and air partition coefficients of volatile organic chemicals*, British J. Indus. Med. 46 (1989), pp. 321–328.
[44] L. Perbellini, F. Brugnone, D. Caretta, and G. Maranelli, *Partition coefficients of some industrial aliphatic hydrocarbons (C5–C7) in blood and human tissues*, British J. Indus. Med. 42 (1985), pp. 162–167.
[45] A. Sato and T. Nakajima, *A structure–activity relationship of some chlorinated hydrocarbons*, Arch. Environ. Health 34 (1979), pp. 69–75.
[46] A. Steward, P.R. Allott, A.L. Cowles, and W.W. Mapleson, *Solubility coefficients for inhaled anaesthetics for water, oil and biological media*, Br. J. Anaesth. 45 (1973), pp. 282–293.
[47] M.H. Abraham, H.S. Chadha, G.S. Whiting, and R.C. Mitchell, *Hydrogen bonding. 32. An analysis of water-octanol and water–alkane partitioning and the delta log P parameter of seiler*, J. Pharm. Sci. 83 (1994), pp. 1085–1100.
[48] M.H. Abraham and P.K. Weathersby, *Hydrogen bonding. 30. Solubility of gases and vapors in biological liquids and tissues*, J. Pharm. Sci. 83 (1994), pp. 1450–1456.
[49] A.L. Cowles, H.H. Borgstedt, and A.J. Gillies, *Solubilities of ethylene, cyclopropane, halothane and diethyl ether in human and dog blood at low concentrations*, Anesthesiology 35 (1971), pp. 203–211.
[50] E.I. Eger II and C.P.J. Larson, *Anaesthetic solubility in blood and tissues: Values and significance*, Br. J. Anaesth. 36 (1964), pp. 140–149.
[51] W. Laass, *Estimation of blood/air partition coefficients of organic solvents*, in *QSAR in Drug Design and Toxicology: Proceedings of the Sixth European Symposium on Quantitative Structure-Activity Relationships*, D. Hadzi and B. Jerman-Blazic, eds., Elsevier, Amsterdam; New York, 1987, pp. 131–134.
[52] R.A. Saraiva, B.A. Willis, A. Steward, J.N. Lunn, and W.W. Mapleson, *Halothane solubility in human blood*, Br. J. Anaesth. 49 (1977), pp. 115–119.
[53] S. Batterman, L. Zhang, S. Wang, and A. Franzblau, *Partition coefficients for the trihalomethanes among blood, urine, water, milk and air*, Sci. Total Environ. 284 (2002), pp. 237–247.
[54] J. DeJongh, H.J. Verhaar, and J.L. Hermens, *A quantitative property–property relationship (QPPR) approach to estimate in vitro tissue–blood partition coefficients of organic chemicals in rats and humans*, Arch. Toxicol. 72 (1997), pp. 17–25.
[55] C.J. Meulenberg and H.P. Vijverberg, *Empirical relations predicting human and rat tissue:air partition coefficients of volatile organic compounds*, Toxicol. Appl. Pharmacol. 165 (2000), pp. 206–216.
[56] C.J. Meulenberg, A.G. Wijnkerm, and H.P. Vijverberg, *Relationship between olive oil:air, saline:air, and rat brain:air partition coefficients of organic solvents in vitro*, J. Toxicol. Environ. Health A 66 (2003), pp. 1985–1998.
[57] S.C. Basak, D. Mills, D.M. Hawkins, and H.A. El-Masri, *Prediction of human blood:air partition coefficient: A comparison of structure-based and property-based methods*, Risk Anal. 23 (2003), pp. 1173–1184.
[58] S.C. Basak, D. Mills, and B.D. Gute, *Prediction of tissue:air partition coefficients – theoretical vs. experimental methods*, SAR QSAR Environ. Res. 17 (2006), pp. 515–532.
[59] F.M. Parham, M.C. Kohn, H.B. Matthews, C. Derosa, and C.J. Portier, *Using structural information to create physiologically based pharmacokinetic models for all polychlorinated biphenyls: I. Tissue:blood partition coefficients*, Toxicol. Appl. Pharmacol. 144 (1997), pp. 340–347.
[60] M.L. Gargas, P.G. Seybold, and M.E. Andersen, *Modeling the tissue solubilities and metabolic rate constant (Vmax) of halogenated methanes, ethanes, and ethylenes*, Toxicol. Lett. 43 (1988), pp. 235–256.

Downloaded by [Montana State University Bozeman] at 08:07 20 August 2014

[61] S.M.J. Free and J.W. Wilson, *A mathematical contribution to structure–activity studies*, J. Med. Chem. 7 (1964), pp. 395–399.
[62] M. Béliveau, R. Tardif, and K. Krishnan, *Quantitative structure–property relationships for physiologically based pharmacokinetic modeling of volatile organic chemicals in rats*, Toxicol. Appl. Pharmacol. 189 (2003), pp. 221–232.
[63] E. Kamgang, T. Peyret, and K. Krishnan, *An integrated QSPR-PBPK modelling approach for in vitro-in vivo extrapolation of pharmacokinetics in rats*, SAR QSAR Environ. Res. 19 (2008), pp. 669–680.
[64] M. Béliveau and K. Krishnan, *A spreadsheet program for modeling of quantitative strucure–pharmacokinetic relationships for inhaled volatile organic chemicals in humans*, SAR QSAR Environ. Res. 16 (2005), pp. 63–77.
[65] P. Poulin and F.P. Theil, *A priori prediction of tissue:plasma partition coefficients of drugs to facilitate the use of physiologically-based pharmacokinetic models in drug discovery*, J. Pharm. Sci. 89 (2000), pp. 16–35.
[66] S. Haddad, P. Poulin, and K. Krishnan, *Relative lipid content as the sole mechanistic determinant of the adipose tissue:blood partition coefficients of highly lipophilic organic chemicals*, Chemosphere 40 (2000), pp. 839–843.
[67] M.P. Payne and L.C. Kenny, *Comparison of models for the estimation of biological partition coefficients*, J. Toxicol. Environ. Health A 65 (2002), pp. 897–931.
[68] T. Peyret, P. Poulin, and K. Krishnan, *A unified algorithm for predicting partition coefficients for PBPK modeling of drugs and environmental chemicals*, Toxicol. Appl. Pharmacol. 249 (2010), pp. 197–207.
[69] P. Poulin and K. Krishnan, *An algorithm for predicting tissue: Blood partition coefficients of organic chemicals from n-octanol: Water partition coefficient data*, J. Toxicol. Environ. Health 46 (1995), pp. 117–129.
[70] P. Poulin and K. Krishnan, *A biologically-based algorithm for predicting human tissue: Blood partition coefficients of organic chemicals*, Hum. Exp. Toxicol. 14 (1995), pp. 273–280.
[71] P. Poulin and K. Krishnan, *A mechanistic algorithm for predicting blood:air partition coefficients of organic chemicals with the consideration of reversible binding in hemoglobin*, Toxicol. Appl. Pharmacol. 136 (1996), pp. 131–137.
[72] P. Poulin and K. Krishnan, *A tissue composition-based algorithm for predicting tissue:air partition coefficients of organic chemicals*, Toxicol. Appl. Pharmacol. 136 (1996), pp. 126–130.
[73] P. Poulin and F.P. Theil, *Prediction of pharmacokinetics prior to in vivo studies. 1. Mechanism-based prediction of volume of distribution*, J. Pharm. Sci. 91 (2002), pp. 129–156.
[74] T. Rodgers, D. Leahy, and M. Rowland, *Physiologically based pharmacokinetic modeling 1: Predicting the tissue distribution of moderate-to-strong bases*, J. Pharm. Sci. 94 (2005), pp. 1259–1276.
[75] T. Rodgers and M. Rowland, *Physiologically based pharmacokinetic modelling 2: Predicting the tissue distribution of acids, very weak bases, neutrals and zwitterions*, J. Pharm. Sci. 95 (2006), pp. 1238–1257.
[76] W. Schmitt, *General approach for the calculation of tissue to plasma partition coefficients*, Toxicol. *In Vitro* 22 (2008), pp. 457–467.
[77] H. Zhang, *A new nonlinear equation for the tissue/blood partition coefficients of neutral compounds*, J. Pharm. Sci. 93 (2004), pp. 1595–1604.
[78] H. Zhang, *A new approach for the tissue–blood partition coefficients of neutral and ionized compounds*, J. Chem. Inf. Model. 45 (2005), pp. 121–127.
[79] H. Zhang and Y. Zhang, *Convenient nonlinear model for predicting the tissue/blood partition coefficients of seven human tissues of neutral, acidic, and basic structurally diverse compounds*, J. Med. Chem. 49 (2006), pp. 5815–5829.
[80] C.-W. Lam, T.J. Galen, J.F. Boyd, and D.L. Pierson, *Mechanism of transport and distribution of organic solvents in blood*, Toxicol. Appl. Pharmacol. 104 (1990), pp. 117–129.

Downloaded by [Montana State University Bozeman] at 08:07 20 August 2014

[81] M. Béliveau, J. Lipscomb, R. Tardif, and K. Krishnan, *Quantitative structure–property relationships for interspecies extrapolation of the inhalation pharmacokinetics of organic chemicals*, Chem. Res. Toxicol. 18 (2005), pp. 475–485.
[82] K. Krishnan and T. Peyret, *Physiologically based toxicokinetic (PBTK) modeling in ecotoxicology*, in *Ecotoxicology Modeling*, J. Devillers, ed., Springer, Dordrecht, 2009, pp. 145–175.
[83] S.L. Bertelsen, A.D. Hoffman, C.A. Gallinat, C.M. Elonen, and J.W. Nichols, *Evaluation of log Kow and tissue lipid content as predictors of chemical partitioning to fish tissues*, Environ. Toxicol. Chem. 17 (1998), pp. 1447–1455.
[84] C. Hansch and A. Leo, *The fragment method of calculating partition coefficients*, in *Substituent Constants for Correlation Analysis in Chemistry and Biology*, C. Hansch and A. Leo, eds., Wiley, New York, 1979, pp. 18–43.
[85] J. Hine and P.K. Mookerjee, *The intrinsic hydrophobic character of organic compounds: Correlations in terms of structural contributions*, J. Org. Chem. 40 (1975), pp. 511–522.
[86] P. Poulin and K. Krishnan, *Molecular structure based prediction of partition coefficients of organic chemicals for physiological pharmacokinetic models*, Toxicol. Meth. 6 (1996), pp. 117–137.
[87] S. Baláž and V. Lukáčová, *A model-based dependence of the human tissue/blood partition coefficients of chemicals on lipophilicity and tissue composition*, Quant. Struct.-Act. Relat. 18 (1999), pp. 361–368.
[88] L.M. Berezhkovskiy, *Volume of distribution at steady state for a linear pharmacokinetic system with peripheral elimination*, J. Pharm. Sci. 93 (2004), pp. 1628–1640.
[89] I. Nestorov, L. Aarons, and M. Rowland, *Quantitative structure–pharmacokinetics relationships: II. A mechanistically based model to evaluate the relationship between tissue distribution parameters and compound lipophilicity*, J. Pharmacokinet. Pharmacodyn. 26 (1998), pp. 521–545.
[90] P. Poulin, K. Schoenlein, and F.-P. Theil, *Prediction of adipose tissue: Plasma partition coefficients for structurally unrelated drugs*, J. Pharm. Sci. 90 (2001), pp. 436–447.
[91] K. Yokogawa, E. Nakashima, J. Ishizaki, H. Maeda, T. Nagano, and F. Ichimura, *Relationships in the structure–tissue distribution of basic drugs in the rabbit*, Pharm. Res. 7 (1990), pp. 691–696.
[92] G. Colmenarejo, *In silico prediction of drug-binding strengths to human serum albumin*, Med. Res. Rev. 23 (2003), pp. 275–301.
[93] G. Colmenarejo, A. Alvarez-Pedraglio, and J.L. Lavandera, *Cheminformatic models to predict binding affinities to human serum albumin*, J. Med. Chem. 44 (2001), pp. 4370–4378.
[94] E. Estrada, E. Uriarte, E. Molina, Y. Simon-Manso, and G.W.A. Milne, *An integrated in silico analysis of drug-binding to human serum albumin*, J. Chem. Inf. Model. 46 (2006), pp. 2709–2724.
[95] N.A. Kratochwil, W. Huber, F. Müller, M. Kansy, and P.R. Gerber, *Predicting plasma protein binding of drugs: A new approach*, Biochem. Pharmacol. 64 (2002), pp. 1355–1374.
[96] J.R. Votano, M. Parham, L.M. Hall, L.H. Hall, L.B. Kier, S. Oloff, and A. Tropsha, *QSAR modeling of human serum protein binding with several modeling techniques utilizing structure-information representation*, J. Med. Chem. 49 (2006), pp. 7169–7181.
[97] C.X. Xue, R.S. Zhang, H.X. Liu, X.J. Yao, M.C. Liu, Z.D. Hu, and B.T. Fan, *QSAR models for the prediction of binding affinities to human serum albumin using the heuristic method and a support vector machine*, J. Chem. Inf. Comput. Sci. 44 (2004), pp. 1693–1700.
[98] S. Coecke, H. Ahr, B.J. Blaauboer, S. Bremer, S. Casati, J. Castell, R. Combes, R. Corvi, C.L. Crespi, M.L. Cunningham, G. Elaut, B. Eletti, A.P. Freidig, A. Gennari, J.-F. Ghersi-Egea, A. Guillouzo, T. Hartung, P. Hoet, M. Ingelman-Sundberg, S. Munn, W. Janssens, B. Ladstetter, D. Leahy, A. Long, A. Meneguz, M. Monshouwer, S. Morath, F. Nagelkerke, O. Pelkonen, J. Ponti, P. Prieto, L. Richert, E. Sabbioni, B. Schaack, W. Steiling, E. Testai, J.-A. Vericat, and A. Worth, *Metabolism: A bottleneck in in vitro toxicological test development. The report and recommendations of ECVAM workshop 54*, Altern. Lab. Anim. 34 (2006), pp. 49–84.

Downloaded by [Montana State University Bozeman] at 08:07 20 August 2014

[99] J.C. Madden and M.T. Cronin, *Structure-based methods for the prediction of drug metabolism*, Expert Opinion Drug Metabol. Toxicol. 2 (2006), pp. 545–557.
[100] R. Mackman, Z. Guo, F.P. Guengerich, and P.R. Ortiz de Montellano, *Active site topology of human cytochrome P450 2E1*, Chem. Res. Toxicol. 9 (1996), pp. 223–226.
[101] D.F.V. Lewis, *On the recognition of mammalian microsomal cytochrome P450 substrates and their characteristics: Towards the prediction of human p450 substrate specificity and metabolism*, Biochem. Pharmacol. 60 (2000), pp. 293–306.
[102] D.F.V. Lewis, *Guide to Cytochromes P450: Structure and Function*, Taylor & Francis, London; New York, 2001.
[103] D.F.V. Lewis, *Quantitative structure–activity relationships (QSARs) within the cytochrome P450 system: QSARs describing substrate binding, inhibition and induction of P450s*, Inflammopharmacology 11 (2003), pp. 43–73.
[104] D.F.V. Lewis and M. Dickins, *Factors influencing rates and clearance in P450-mediated reactions: QSARs for substrates of the xenobiotic-metabolizing hepatic microsomal P450s*, Toxicology 170 (2002), pp. 45–53.
[105] D.F.V. Lewis, Y. Ito, and B.G. Lake, *Quantitative structure–activity relationships (QSARs) for inhibitors and substrates of CYP2B enzymes: Importance of compound lipophilicity in explanation of potency differences*, J. Enzyme Inhib. Med. Chem. 25 (2010), pp. 679–684.
[106] H. Li, J. Sun, X. Sui, J. Liu, Z. Yan, X. Liu, Y. Sun, and Z. He, *First-principle, structure-based prediction of hepatic metabolic clearance values in human*, Eur. J. Med. Chem. 44 (2009), pp. 1600–1606.
[107] K. Nikolic and D. Agababa, *Prediction of hepatic microsomal intrinsic clearance and human clearance values for drugs*, J. Mol. Graph. Model. 28 (2009), pp. 245–252.
[108] R.P. Austin, P. Barton, S.L. Cockroft, M.C. Wenlock, and R.J. Riley, *The influence of nonspecific microsomal binding on apparent intrinsic clearance, and its prediction from physicochemical properties*, Drug Metab. Dispos. 30 (2002), pp. 1497–1503.
[109] R.P. Austin, P. Barton, S. Mohmed, and R.J. Riley, *The binding of drugs to hepatocytes and its relationship to physicochemical properties*, Drug Metab. Dispos. 33 (2005), pp. 419–425.
[110] H. Yin, M.W. Anders, K.R. Korzekwa, L.A. Higgins, K.T. Thummel, E.D. Kharasch, and J.P. Jones, *Designing safer chemicals: Predicting the rates of metabolism of halogenated chemicals*, Proc. Natl. Acad. USA 92 (1995), pp. 11076–11080.
[111] G.D. Loizou, N.L. Eldirdiri, and L.J. King, *Physiologically based pharmacokinetics of uptake by inhalation of a series of 1,1,1-trihaloethanes: Correlation with various physicochemical parameters*, Inhal. Toxicol. 8 (1996), pp. 1–19.
[112] M.L. Gargas, H.J. Clewell, and M.E. Andersen, *Gas uptake inhalation techniques and the rates of metabolism of chloromethanes, chloroethanes and chloroethylenes in the rat*, Inhal. Toxicol. 2 (1990), pp. 295–319.
[113] B. Mortensen, I. Eide, K. Zahlsen, and O.G. Nilsen, *Prediction of in vivo metabolic clearance of 25 different petroleum hydrocarbons by a rat liver head-space technique*, Arch. Toxicol. 74 (2000), pp. 308–312.
[114] G. Galliani, B. Rindone, G. Dagnino, and M. Salmona, *Structure reactivity relationships in the microsomal oxidation of tertiary amines*, Eur. J. Drug Metabol. Pharm. 9 (1984), pp. 289–293.
[115] G.A. Csanady, R.J. Laid, and J.G. Filser, *Metabolic transformation of halogenated and other alkenes – a theoretical approach. Estimation of metabolic reactivities for in vivo conditions*, Toxicol. Lett. 75 (1995), pp. 217–223.
[116] F.M. Parham and C.J. Portier, *Using structural information to create physiologically based pharmacokinetic models for all polychlorinated biphenyls. II. Rates of metabolism*, Toxicol. Appl. Pharmacol. 151 (1998), pp. 110–116.
[117] D.F. Lewis, C. Sams, and G.D. Loizou, *A quantitative structure–activity relationship analysis on a series of alkyl benzenes metabolized by human cytochrome P450 2E1*, J. Biochem. Mol. Toxicol. 17 (2003), pp. 47–52.

Downloaded by [Montana State University Bozeman] at 08:07 20 August 2014

[118] J.B. Knaak, C.C. Dary, F. Power, C. Thompson, and J.N. Blancato, *Physicochemical and biological data for the development of predictive organophosphorus pesticide QSARs and PBPK/PD models for human risk assessment*, Crit. Rev. Toxicol. 34 (2004), pp. 143–207.
[119] C.L. Waller, M.V. Evans, and J.D. McKinney, *Modeling the cytochrome P450-mediated metabolism of chlorinated volatile organic compounds*, Drug Metab. Dispos. 24 (1996), pp. 203–210.
[120] P. Poulin and K. Krishnan, *Molecular structure-based prediction of the toxicokinetics of inhaled vapors in humans*, Int. J. Toxicol. 18 (1999), pp. 7–18.
[121] G.R. Wilkinson and D.G. Shand, *Commentary: A physiological approach to hepatic drug clearance*, Clin. Pharmacol. Ther. 18 (1975), pp. 377–390.
[122] M.E. Andersen, *A physiologically based toxicokinetic description of the metabolism of inhaled gases and vapors: Analysis at steady state*, Toxicol. Appl. Pharmacol. 60 (1981), pp. 509–526.
[123] G.E. Blakey, I.A. Nestorov, P.A. Arundel, L.J. Aarons, and M. Rowland, *Quantitative structure–pharmacokinetics relationships: I. Development of a whole-body physiologically based model to characterize changes in pharmacokinetics across a homologous series of barbiturates in the rat*, J. Pharmacokinet. Pharmacodyn. 25 (1997), pp. 277–312.
[124] T. Yamagushi, M. Yabuki, S. Saito, T. Watanabe, H. Nishimura, N. Isobe, F. Shono, and M. Matsuo, *Research to develop a predicting system of mammalian subacute toxicity (3) construction of a predictive toxicokinetic model*, Chemosphere 33 (1996), pp. 2441–2468.
[125] B. Agoram, W.S. Woltosz, and M.B. Bolger, *Predicting the impact of physiological and biochemical processes on oral drug bioavailability*, Adv. Drug Deliv. Rev. 50 (2001), pp. S41–S67.
[126] P.V. Balimane, S. Chong, and R.A. Morrison, *Current methodologies used for evaluation of intestinal permeability and absorption*, J. Pharmacol. Toxicol. Methods 44 (2000), pp. 301–312.
[127] G.M. Grass and P.J. Sinko, *Physiologically-based pharmacokinetic simulation modelling*, Adv. Drug Deliv. Rev. 54 (2002), pp. 433–451.
[128] H. Patel, W. ten Berge, and M.T. Cronin, *Quantitative structure–activity relationships (QSARs) for the prediction of skin permeation of exogenous chemicals*, Chemosphere 48 (2002), pp. 603–613.
[129] P. Poulin and K. Krishnan, *Molecular structure-based prediction of human abdominal skin permeability coefficients for several organic compounds*, J. Toxicol. Environ. Health A 62 (2001), pp. 143–159.
[130] O.A. Raevsky and K.-J. Schaper, *Quantitative estimation of hydrogen bond contribution to permeability and absorption processes of some chemicals and drugs*, Eur. J. Med. Chem. 33 (1998), pp. 799–807.
[131] O.A. Raevsky, S.V. Trepalin, H.P. Trepalina, V.A. Gerasimenko, and O.E. Raevskaja, *SLIPPER-2001 – Software for predicting molecular properties on the basis of physicochemical descriptors and structural similarity*, J. Chem. Inf. Comput. Sci. 42 (2002), pp. 540–549.
[132] M. Debia and K. Krishnan, *Quantitative property–property relationships for computing occupational exposure limits and vapour hazard ratios of organic solvents*, SAR QSAR Environ. Res. 21 (2010), pp. 583–601.

Downloaded by [Montana State University Bozeman] at 08:07 20 August 2014